

This is a repository copy of *Polyamines are required for normal growth in sinorhizobium meliloti*.

White Rose Research Online URL for this paper:

<https://eprints.whiterose.ac.uk/130198/>

Version: Accepted Version

---

**Article:**

Becerra-Rivera, Victor A., Bergström, Ed, Thomas-Oates, Jane [orcid.org/0000-0001-8105-9423](https://orcid.org/0000-0001-8105-9423) et al. (1 more author) (2018) Polyamines are required for normal growth in *sinorhizobium meliloti*. *Microbiology* (Reading, England). 000615. pp. 600-613. ISSN 1465-2080

<https://doi.org/10.1099/mic.0.000615>

---

**Reuse**

Items deposited in White Rose Research Online are protected by copyright, with all rights reserved unless indicated otherwise. They may be downloaded and/or printed for private study, or other acts as permitted by national copyright laws. The publisher or other rights holders may allow further reproduction and re-use of the full text version. This is indicated by the licence information on the White Rose Research Online record for the item.

**Takedown**

If you consider content in White Rose Research Online to be in breach of UK law, please notify us by emailing [eprints@whiterose.ac.uk](mailto:eprints@whiterose.ac.uk) including the URL of the record and the reason for the withdrawal request.

1 Polyamines are required for normal growth in *Sinorhizobium meliloti*

2

3

4 Victor A. Becerra-Rivera<sup>1</sup>, Ed Bergström<sup>2</sup>, Jane Thomas-Oates<sup>2</sup> and Michael F.  
5 Dunn<sup>1\*</sup>

6

7

8 **Author affiliations:** <sup>1</sup>Programa de Genómica Funcional de Procariotes, Centro de  
9 Ciencias Genómicas, Universidad Nacional Autónoma de México, Cuernavaca,  
10 Morelos 62210, Mexico. <sup>2</sup>Centre of Excellence in Mass Spectrometry and  
11 Department of Chemistry, University of York, Heslington, York, YO10 5DD, UK.

12 **\*Correspondence:** Michael F. Dunn, mike@ccg.unam.mx

13 **Key words:** *S. meliloti*; polyamines; putrescine; spermidine; homospermidine;  
14 norspermidine; ornithine decarboxylase

15 **Abbreviations:** ADC, arginine decarboxylase; Agm, agmatine; Arg, L-arginine; L-  
16 Asp β-SA, L-aspartate β-semialdehyde; Cad, cadaverine; Cb, carbenicillin; CID,  
17 collision induced dissociation; DAP, 1,3-diaminopropane; DNS, dansyl group;  
18 DNSCl, dansyl chloride; DNS-PA, dansyl-polyamine; FT-ICR, Fourier-transform ion  
19 cyclotron resonance; Gm, gentamicin; Gus, β-glucuronidase; *gusA*, gene encoding  
20 β-glucuronidase; HPTLC, high performance thin layer chromatography; HSpd,  
21 homospermidine; Km, kanamycin; LB, Luria-Bertani; Lys, L-lysine; LDC, lysine  
22 decarboxylase; MALDI, matrix-assisted laser desorption/ionisation; MMS, minimal  
23 medium succinate-ammonium; MMS-acid, MMS medium, pH 5.5; MMS-Salt, MMS  
24 medium with 0.3 M NaCl; MS, mass spectrometry; MS/MS, tandem mass  
25 spectrometry; μ, generations h<sup>-1</sup>; Nm neomycin; NSpd, norspermidine; OD<sub>600</sub>,  
26 optical density at 600 nm; ODC, ornithine decarboxylase; *odc1*, gene encoding  
27 ornithine decarboxylase SMa0680; *odc2*, gene encoding lysine/ornithine  
28 decarboxylase SMc02983; Orn, L-ornithine; PA, polyamine; Put, putrescine; PY,  
29 peptone-yeast extract; Sp, spectinomycin; Spd, spermidine; Spm, spermine; Sm,  
30 streptomycin; TCA, trichloroacetic acid; TSS, transcriptional start site.

31 One supplementary table and one supplementary figure are available with the  
32 online Supplementary Material.

33 **Subject category:** Physiology and metabolism

34 **Word count:** 6,279

35

36 **Abstract**

37 Polyamines (PAs) are ubiquitous polycations derived from basic L-amino acids  
38 whose physiological roles are still being defined. Their biosynthesis and functions  
39 in nitrogen-fixing rhizobia such as *Sinorhizobium meliloti* have not been extensively  
40 investigated. Thin layer chromatographic and mass spectrometric analyses  
41 showed that *S. meliloti* Rm8530 produces the PAs putrescine (Put), spermidine  
42 (Spd) and homospermidine (HSpd) in their free forms and norspermidine (NSpd) in  
43 a form bound to macromolecules. The *S. meliloti* genome encodes two putative  
44 ornithine decarboxylases (ODC) for Put synthesis. Activity assays with the purified  
45 enzymes showed that ODC2 (SMc02983) decarboxylates both ornithine and  
46 lysine. ODC1 (SMa0680) decarboxylates only ornithine. An *odc1* mutant was  
47 similar to the wild type in ODC activity, PA production and growth. In comparison  
48 to the wild type, an *odc2* mutant had 45 % as much ODC activity and its growth  
49 rates were reduced by 42, 14 and 44 % under non-stress, salt stress or acid stress  
50 conditions, respectively. The *odc2* mutant produced only trace levels of Put, Spd  
51 and HSpd. Wild type phenotypes were restored when the mutant was grown in  
52 cultures supplemented with 1 mM Put or Spd or when the *odc2* gene was  
53 introduced *in trans*. *odc2* gene expression was increased under acid stress and  
54 reduced under salt stress and with exogenous Put or Spd. An *odc1 odc2* double  
55 mutant had phenotypes similar to the *odc2* mutant. These results indicate that  
56 ODC2 is the major enzyme for Put synthesis in *S. meliloti* and that PAs are  
57 required for normal growth *in vitro*.

58

59 **INTRODUCTION**

60 Polyamines (PAs) are low molecular weight organic compounds with two or more  
61 amino groups that are positively charged at neutral pH [1]. With few exceptions,  
62 PAs are ubiquitous in all organisms and have important roles in processes as  
63 diverse as growth, stress resistance and the regulation of transcription and  
64 translation in both eukaryotes and prokaryotes [2-5]. In contrast to their essential  
65 functions in eukaryotes and archaea, the physiological roles of PAs in bacteria are  
66 less clearly defined. In prokaryotes, PAs are involved in biofilm formation, stress

67 resistance, motility, pathogenesis, and growth. [6-12]. This diversity of functions  
68 might explain the presence of the more varied PA repertoire in bacteria [5].

69

70 Diamines found in bacteria include putrescine (Put), cadaverine (Cad) and 1,3-  
71 diaminopropane (DAP) (Fig. 1). Put is produced by nearly all bacteria, Cad is  
72 common in Proteobacteria and DAP is found sporadically in diverse phyla.  
73 Spermidine (Spd) is the most commonly found triamine, though bacteria may  
74 produce the related homospermidine (HSpd) and/or, less commonly,  
75 norspermidine (NSpd) [2,5,13].

76

77 Put can be made by the decarboxylation of L-ornithine (Orn) by Orn decarboxylase  
78 (ODC; EC 4.1.1.17) or of L-arginine (Arg) by Arg decarboxylase (ADC; EC  
79 4.1.1.19). The ADC reaction produces agmatine (Agm), which is converted to Put  
80 by agmatinase (SpeB; EC 3.5.3.11). Cad is produced by lysine decarboxylase  
81 (LDC; EC 4.1.1.18) acting on L-lysine (Lys). Some decarboxylases have activity  
82 with both Lys and Orn as substrates [5,13,14].

83

84 In *Sinorhizobium meliloti* and other nitrogen-fixing rhizobia, work on PAs has  
85 focused on their identification and quantification during free-living growth [15,16],  
86 changes in their levels *in nodulo* when host plants were subjected to abiotic stress,  
87 or determining the effects of exogenous polyamines on symbiosis [12,17-21]. A  
88 few studies using biochemical and genetic approaches have shown species-  
89 dependent requirements for different PAs for growth, biofilm formation and motility  
90 in rhizobia [11,22-25].

91

92 Three studies with different strains of *S. meliloti* grown in minimal medium show  
93 that its free PA fraction invariably contains Put, Spd and HSpd, with Cad found in  
94 two of the studies [15,16,19]. Hamana et al. [16] assayed for, but did not detect,  
95 Agm, spermine (Spm), NSpd or DAP in *S. meliloti* IAM 12611. PAs in *S. meliloti*  
96 1021 have been reported only for cultures grown in rich medium, where Put, Spd,  
97 HSpd and Spm were detected [19]; the latter probably originates from Spm present

98 in the tryptone and yeast extract components of the medium [14]. In contrast to  
99 other rhizobia, the genome sequence of strain 1021 indicates that it is able to  
100 synthesize NSpd, which has not been reported in rhizobia, and possesses an  
101 "alternative" pathway for Spd synthesis [14]. The strain 1021 genome encodes  
102 three putative basic amino acid decarboxylases. *sma0682* is annotated as a  
103 "decarboxylase (lysine, ornithine, arginine)" but its genomic context and sequence  
104 suggest that it encodes an ADC. We predicted that *sma0680* (annotated as "amino  
105 acid (ornithine, lysine, arginine) decarboxylase") encodes an ODC: we denominate  
106 this gene and enzyme as *odc1* and ODC1, respectively. *smc02983* is annotated as  
107 an "ornithine, DAP, or arginine decarboxylase" but its product has sequence  
108 characteristics that suggest it is able to decarboxylate both lysine and ornithine  
109 [14,26]. We refer here to the *smc02983* gene and protein product as *odc2* and  
110 ODC2, respectively (Fig. 1).

111

112 Because *S. meliloti* has multiple enzymes catalyzing the conversion of *N*-  
113 acetylornithine to Orn during Arg biosynthesis [27] and is also able to produce Orn  
114 with an inducible arginase [14,26], we hypothesized that Orn is the major precursor  
115 for Put synthesis in this organism [27]. If this is correct, then ODC1 and/or ODC2  
116 should be the key enzyme(s) for the synthesis of Put and the PAs derived from it  
117 (Fig. 1). The work presented here shows that ODC2 is responsible for synthesizing  
118 the majority of the Put produced by *S. meliloti* and that PAs are important for  
119 normal growth in minimal medium cultures with and without abiotic stress.

120

## 121 **METHODS**

### 122 **Bacterial strains, plasmids and culture growth conditions**

123 Bacterial strains and plasmids are listed in Table 1. PY and LB complex media,  
124 and MMS minimal medium with succinate and NH<sub>4</sub>Cl as carbon and nitrogen  
125 sources, respectively, were described previously [27]. Salt stress was caused by  
126 growing cultures in MMS-salt medium, where NaCl was added to MMS to a final  
127 concentration of 0.3 M before adjusting the pH to 6.8 and autoclaving. For growth  
128 under acidic stress, MMS-acid medium was prepared by adjusting MMS medium to

129 pH 5.5 (rather than 6.8) before autoclaving. PA and amino acid supplements were  
130 prepared as 0.5 M stocks, adjusted to pH 6.8 (for use in MMS and MMS-salt) or pH  
131 5.5 (for use in MMS-acid) and filter sterilized. To grow *S. meliloti* strains, cells from  
132 3 day PY plates with appropriate antibiotics were used to inoculate 3 ml of liquid  
133 PY containing the same antibiotics and incubated at 200 rpm, 30°C. After 24 h, 1  
134 ml of these cultures were used to inoculate 50 ml of PY containing one-half the  
135 normal concentration of antibiotics, in 125 ml baffled flasks. These cultures were  
136 incubated as above for 24 h, harvested by centrifugation at 5500 x g for 5 min, the  
137 cells washed twice in MMS and resuspended to an OD<sub>600</sub> of approximately 1.5 in  
138 MMS. These suspensions were used to inoculate the desired minimal medium  
139 without antibiotics to an initial OD<sub>600</sub> of 0.05: for transcriptional fusion and PA  
140 analyses, respectively, the medium:baffled flask volume ratios were 50:125 ml and  
141 100:250 ml. Cultures were grown with agitation at 200 rpm at 30°C and growth  
142 was monitored at 600 nm. Specific growth rates ( $\mu$ , generations h<sup>-1</sup>) were  
143 calculated [28] from culture OD<sub>600</sub> values obtained between 4 and 12 h under non-  
144 stress conditions and 4 to 24 h under stress conditions. When required, antibiotics  
145 were used at the following concentrations ( $\mu\text{g ml}^{-1}$ ): carbenicillin (Cb), 50;  
146 gentamicin (Gm), 15; kanamycin (Km), 50; neomycin (Nm), 60; spectinomycin  
147 (Sp), 100; streptomycin (Sm), 200.

148

### 149 **DNA manipulations**

150 Standard protocols were used to grow *E. coli* and for DNA isolation, restriction  
151 digests, cloning and transformation [29]. Bacterial conjugations were performed as  
152 described previously [27]. High-stringency DNA hybridizations were done with a  
153 DIG-High Prime DNA Labeling kit (Roche).

154

155

156 **PCR amplifications**

157 DNA sequences were obtained from GenBank ([www.ncbi.nlm.nih.gov/gene/](http://www.ncbi.nlm.nih.gov/gene/)).  
158 Primers (Table S1, Supplementary material) were used in PCR reactions with  
159 Accuprime Taq DNA polymerase (Invitrogen) to clone genes for the construction of  
160 transcriptional fusions or whose products were to be overexpressed and purified,  
161 or with Dream Taq PCR master mix (Thermo) for other purposes. PCR cycling  
162 programs included a denaturing step at 95°C for 1 min followed by 30 cycles of  
163 95°C for 1 min, 56°C for 1 min and 72°C for a time appropriate for the length of the  
164 DNA being amplified. A final elongation step was made at 72°C for 10 min. For  
165 use in cloning, PCR products were purified with a commercially available kit.

166

167 **Recombinant protein purification**

168 *S. meliloti* genes *odc1* and *odc2* were amplified by PCR (Table S1) and cloned in  
169 pET Sumo to generate plasmids pSumo-*odc1* and pSumo-*odc2* (Table 1). These  
170 plasmids were used to overexpress the corresponding 6His-Sumo tagged protein  
171 products in *E. coli* BL21(DE3). For overexpression and purification, strain  
172 BL21(DE3) transformed with either pSumo-*odc1* or pSumo-*odc2* were grown in  
173 100 ml LB Km at 37°C, 200 rpm to an OD<sub>600</sub> of 0.4, IPTG was added to a final  
174 concentration of 1 mM and incubation continued for 8 and 14 h, respectively. 6His-  
175 Sumo tagged proteins were purified using Ni-NTA resin (Invitrogen) under hybrid  
176 conditions following the manufacturer's protocol.

177

178 **Mutant construction**

179 Mutants of *S. meliloti* Rm8530 were constructed by the insertional inactivation of  
180 genes as described previously [27]. Briefly, genome regions encoding *odc1* and  
181 *odc2* were amplified by PCR (Table S1) and cloned into pCR 2.1-Topo to produce  
182 plasmids pCRodc1 and pCRodc2 (Table 1). Following verification by restriction  
183 enzyme analysis, the inserts from pCRodc1 and pCRodc2 were excised with  
184 *SmaI/XbaI* and *SaII*, respectively, and inserted into suicide vector pK18mobsacB  
185 cut with *SmaI/XbaI* or *XhoI* to give plasmids pKodc1 and pKodc2 respectively. The  
186 loxP Sp cassette from pMS102loxSp17 was ligated into the *Bam*HI and *SaII* sites

187 of the genes cloned in pKodc1 and pKodc2, respectively, generating plasmids  
188 pKodc1::loxSp and pKodc2::loxSp (Table 1). These constructs were introduced  
189 into *S. meliloti* Rm8530 by triparental mating using *E. coli* DH5 $\alpha$ /pRK2013 as  
190 helper. A Sp<sup>r</sup> Nm<sup>r</sup> single recombinant obtained from each mating was spread on  
191 PY containing Sm, Sp and 12 % sucrose to allow the selection of the 8530 *odc1*  
192 and 8530 *odc2* mutants (Table 1). The 8530 *odc1 odc2* double mutant was  
193 constructed in two steps. First, the loxP Sp interposon in the *odc1* gene in the 8530  
194 *odc1* mutant was deleted by introducing plasmid pBBRMCre, which expresses the  
195 loxP-specific Cre recombinase, into the mutant. The desired loxP Sp deletion and  
196 pBBRMCre plasmid-cured strain was selected by screening for the Sm<sup>r</sup> Sp<sup>s</sup> and  
197 Sm<sup>r</sup> Gm<sup>s</sup> phenotypes, respectively [30]. In the second step, plasmid pKodc2::loxSp  
198 was introduced into the 8530 *odc1* loxSp-deleted mutant to obtain the 8530 *odc1*  
199 *odc2* double mutant by selection for sucrose sensitivity. The correct construction of  
200 the mutants was confirmed by Southern hybridization.

201

### 202 **Genetic complementation of the 8530 *odc2* mutant**

203 To test genetic complementation of the *odc2* mutant, we excised the *EcoRI*  
204 fragment from pCRodc2, which contains the *odc2* gene with its native promoter  
205 and terminator regions, and introduced it into pBB5 to give plasmid pBB5-*odc2*.  
206 This plasmid, or pBB5 without an insert, was introduced into the 8530 *odc2* mutant  
207 by triparental mating.

208

### 209 **Basic amino acid decarboxylase assays**

210 The radiochemical assay for determining ODC activity in intact cells was modified  
211 from that of Romano et al. [31]. Cells from 16 h cultures were washed twice with  
212 100 mM potassium phosphate buffer, pH 7 (KP 7) and resuspended to an OD<sub>600</sub> of  
213 3.0. Assay mixtures (250  $\mu$ l) contained 100 mM KP 7, 4.5 mM MgSO<sub>4</sub>, 3 mM  $\beta$ -  
214 mercaptoethanol and 85 nM pyridoxal-5'-phosphate. Individual reactions were  
215 started by adding L-ornithine to a final concentration of 3.5 mM containing 0.025  
216  $\mu$ Ci of L-[1-<sup>14</sup>C]-ornithine. Assay mixtures were deposited in plastic tubes in which  
217 a CO<sub>2</sub> trap consisting of a 2 x 2.5 cm piece of filter paper wet with 125  $\mu$ l of 1 M



218 NaOH was placed so as to adhere to the top portion of the tube. Fifty  $\mu\text{l}$  aliquots of  
219 cell suspension were added to the tubes, which were sealed with rubber septa and  
220 incubated for 4 h at 30°C. Reactions were stopped by adding 200  $\mu\text{l}$  of 10 %  
221 trichloroacetic acid (TCA) and samples were re-capped and left at room  
222 temperature for one hour. The paper CO<sub>2</sub> traps were mixed with 10 ml of Ultima  
223 Gold LSC cocktail (Sigma) and radioactivity determined by liquid scintillation  
224 counting. One unit (U) of activity is defined as the production of 1 nmol CO<sub>2</sub> min<sup>-1</sup>  
225 mg protein<sup>-1</sup>. Total cellular protein was determined as described previously [32].  
226 Decarboxylase activities of the purified 6His-Sumo-ODC1 or 6His-Sumo-ODC2  
227 enzymes were determined using colorimetric assays with Arg [33], Orn [34] or Lys  
228 [35] as substrates. Assay of purified enzymes was done using 25-30  $\mu\text{g}$  of purified  
229 6His-Sumo-ODC1 or 6His-Sumo-ODC2 per reaction and 1 U of activity is defined  
230 as the production of 1 nmol of decarboxylation product min<sup>-1</sup> mg protein<sup>-1</sup>. Protein  
231 concentrations were determined by the Bradford method [36].

232

### 233 **Construction of a *odc2* transcriptional fusion with the $\beta$ -glucuronidase** 234 **(*gusA*) gene**

235 *odc2* is the first gene of a predicted two gene operon but does not contain a  
236 predicted transcription start site (TSS) [37]. The PCR primers used to amplify the  
237 upstream and 5' coding region of *odc2* are described in Table S1, and the  
238 amplified region was cloned into pTZ57R/T (Table 1). The *gusA* fusion with this  
239 gene, plasmid pBB53odc2::*gusA*, was constructed using the PCR product of *odc2*  
240 that includes the 586 nt intergenic region between its start codon and that of the  
241 divergently transcribed *smc02984* gene, 19 and 297 nt of the of the *smc02984* and  
242 *odc2* coding regions, respectively. A clone containing the pTZ57R/T plasmid with  
243 the PCR product in the desired orientation was identified by digestion with  
244 appropriate restriction enzymes. The insert from the plasmid was excised with  
245 *Apal/XbaI* and cloned into vector pBBMCS-53 cut likewise, transcriptionally fusing  
246 the *odc2* promoter/5' region to the *gusA* gene. The correct transcriptional  
247 orientation of the fusion plasmid was confirmed by restriction enzyme digestion and  
248 in PCR reactions with primer p53lw (reverse primer specific for *gusA*) and the

249 forward primer for *odc2* (Table S1; [27]). The fusion plasmid was transferred to *S.*  
250 *meliloti* Rm8530 by triparental mating.

251

### 252 **$\beta$ -glucuronidase (Gus) assays**

253 Experimental cultures were grown in the desired minimal medium for 16 h at 30°C  
254 with shaking at 200 rpm. Gus activity was determined by measuring the production  
255 of *p*-nitrophenol from the *p*-nitrophenyl  $\beta$ -D-glucuronide substrate with quantitation  
256 based on total protein [27]. One unit (U) of activity is defined as the production of 1  
257 nmol of product min<sup>-1</sup> mg protein<sup>-1</sup>. Strain Rm8530 containing pBBMCS-53 without  
258 an insert lacked Gus activity under the growth conditions tested.

259

### 260 **Polyamine analysis by High Performance Thin-Layer Chromatography** 261 **(HPTLC)**

262 Dansyl (DNS) derivatives of PAs were analyzed by HPTLC using modifications of  
263 previously published protocols [38,39]. Cells from 32 h cultures were pelleted by  
264 centrifugation at 5500 x *g* for 5 min and resuspended to an OD<sub>600</sub> of 3.0 in fresh  
265 MMS. Cells from 1 ml portions of these suspensions were pelleted at 13,200 x *g*,  
266 resuspended with 0.5 ml of 5 % (w/v) TCA and stored at 4°C for 18-24 h. Free  
267 PAs present in the TCA supernatants, obtained by centrifugation at 13,200 x *g* for  
268 10 min, were derivatized in 2 ml glass vials by mixing 40  $\mu$ l of the supernatant, 80  
269  $\mu$ l of dansyl-chloride (DNSCI) solution (5 mg ml<sup>-1</sup> in acetone) and 40  $\mu$ l of  
270 supersaturated aqueous sodium carbonate. Reaction mixtures containing PA  
271 standards (1.2  $\mu$ g of the PA in 40  $\mu$ l of 5 % TCA) were derivatized in the same way.  
272 The capped vials were heated at 80°C for 1 h, cooled to room temperature and  
273 quenched with 20  $\mu$ l of L-proline solution (150 mg ml<sup>-1</sup> in water) for 30 min at room  
274 temperature in darkness. The reaction mixtures were extracted twice with 100  $\mu$ l of  
275 toluene and the combined extracts dried under a stream of N<sub>2</sub>. Samples of DNS-  
276 PA standards and DNS-PAs from cells were resuspended with 100 and 45  $\mu$ l of  
277 toluene, respectively. One  $\mu$ l of DNS-PA standards or 10  $\mu$ l of DNS-PAs from cells  
278 were run on Silica Gel 60 HPTLC plates (Merck) using chloroform/triethylamine  
279 (5:1 v/v) as mobile phase. For the routine determination of PAs produced by *S.*

280 *meliloti* cells from cultures, only the free PA fraction was analyzed. PAs can exist  
281 as free molecules in the cytoplasm or as forms bound to macromolecules such as  
282 proteins, lipids or nucleic acids. These bound forms of PAs can be obtained in  
283 their free forms by strong acid hydrolysis of the TCA-precipitated macromolecules  
284 [14]. We analyzed PAs bound to macromolecules as follows. Pellets of insoluble  
285 material obtained from treating cells with 5 % TCA were washed with 0.5 ml of 5 %  
286 TCA and the pellets resuspended with 0.5 ml of 6 N HCl. The suspensions were  
287 heated at 110°C for 18-24 h in 2 ml V-Vials with teflon-lined caps (Sigma). Twenty  
288 µl of hydrolysate was combined with 40 µl each of the DNSCI and supersaturated  
289 sodium carbonate solutions described above, and derivatization and HPTLC  
290 carried out as for free PAs. Plates were visualized under UV light and images  
291 captured with a Syngene (Frederick, MD, USA) InGenius imaging system.  
292 Densitometric quantification was done using ImageJ 1.48v software. For mass  
293 spectrometric analysis, the silica gel corresponding to DNS-PA spots were scraped  
294 off the TLC plates and eluted with methanol. After passage through 0.22 µM  
295 cellulose acetate filter units (Costar), methanol was removed under a N<sub>2</sub> stream.  
296 The samples were reconstituted in 200 µl acetonitrile:H<sub>2</sub>O (1:1; v:v) containing  
297 0.25% (v:v) formic acid.

298

### 299 **Mass spectrometric analysis of dansyl-PAs**

300 MALDI mass spectra were acquired using a Bruker 9.4T solariX XR Fourier-  
301 transform ion cyclotron resonance (FT-ICR) mass spectrometer (Bremen,  
302 Germany). The samples were ionized in positive ion mode using the MALDI ion  
303 source with α-cyano-4-hydroxycinnamic acid (CHCA) matrix. Sample spots were  
304 produced by premixing 1.4 µl of sample solution with the same volume of matrix  
305 solution (saturated solution in acetonitrile:H<sub>2</sub>O (1:1; v:v) containing 0.25% (v:v)  
306 formic acid); 1 µl of this mixture was spotted onto a stainless steel target plate and  
307 allowed to air dry at ambient temperature. Spectra were measured with a transient  
308 length of 2.2 s resulting in a resolving power of 400000 at *m/z* 400. The instrument  
309 was externally calibrated using a standard peptide mix and a 'lock-mass' calibration  
310 was used with the matrix ion with *m/z* 568.135. Collision induced dissociation

311 (CID) was used to generate product ions and was achieved in the hexapole  
312 collision cell using argon as the collision gas. Product ion spectra were recorded  
313 with a transient length of 1.1 s, giving a resolution of 200000 at  $m/z$  400.

314

## 315 **RESULTS AND DISCUSSION**

### 316 **Identification of PAs produced by *S. meliloti* Rm8530**

317 The work reported here uses *S. meliloti* Rm8530 as wild type. This strain is  
318 identical to the sequenced and well-characterized strain 1021 except that it has a  
319 functional copy of the *expR* gene, whose product is involved in quorum-sensing  
320 based transcriptional regulation [40]. PA production by strain Rm8530 has not  
321 been reported previously. By HPTLC analysis, we found no quantitative or  
322 qualitative differences in the PAs produced by strains 1021 and Rm8530 grown  
323 under the conditions reported here (results not shown).

324

325 Selected *S. meliloti* dansyl-PA (DNS-PA) derivatives and DNS-derivatives of  
326 authentic PA standards were isolated from HPTLC plates (Fig. S1 (a),  
327 Supplementary material) and analyzed by MALDI high resolution, high mass  
328 accuracy FT-ICR mass spectrometry (MS) and product ion tandem mass  
329 spectrometry (MS/MS). The details of this analysis are described in Fig. S1,  
330 Supplementary material. The reason for this analysis was to unambiguously identify  
331 DNS-PA spots present on our HPTLC plates, and this was particularly important for  
332 HSpd, for which no commercial standard is available, and for NSpd, which has not  
333 been reported in rhizobia.

334

335 As mentioned, PA analyses of various *S. meliloti* grown in culture showed the  
336 presence of Put, Spd, HSpd and (usually) Cad, but not Agm, spermine (Spm),  
337 NSpd or DAP. Our analysis of the PAs produced by strain Rm8530 grown in MMS  
338 (Fig. S1) shows the presence of Put, Spd, HSpd and NSpd, with the latter found  
339 only in the bound PA fraction. The presence of NSpd only in the bound fraction  
340 explains why it has not been detected previously in *S. meliloti*. Our results also  
341 indicate that Cad (or a Cad-like compound) is produced. We tentatively identified

342 DAP in cells from PA-supplemented cultures (described later), while neither Agm  
343 nor Spm were detected under any growth condition (results not shown).

344

#### 345 **Amino acids decarboxylated by ODC1 and ODC2**

346 To provide a biochemical basis for our assignment of the ODC1 and ODC2  
347 proteins as a monofunctional ODC and a bifunctional Lys/ODC, respectively, we  
348 purified each as 6His-Sumo-tagged proteins and tested their ability to  
349 decarboxylate Arg, Lys and Orn. Neither protein had detectible activity with Arg as  
350 substrate. With Orn, the 6His-Sumo-ODC1 had a specific activity of 4.1 U, but no  
351 activity with Lys as substrate. The 6His-Sumo-ODC2 had specific activities of 8.6  
352 and 0.9 U using Orn and Lys, respectively, as substrates. These results match our  
353 prediction of the substrates decarboxylated by each enzyme [14].

354

#### 355 **ODC2 is the major enzyme for Put synthesis in *S. meliloti***

356 To determine the importance of ODC1 and ODC2 in PA synthesis, we constructed  
357 single and double mutants of strain Rm8530 in which the encoding gene(s) were  
358 inactivated (Table 1). Because both the *odc1* and *odc2* genes are present in  
359 operons [37], the inactivation of either gene probably also prevents the  
360 transcription of downstream gene(s) in the operons. For *odc1*, the downstream  
361 genes encode a Put transporter (PotE; SMa0678) and a ABC transporter substrate  
362 binding protein possibly for glutamate/aspartate (SMa0677). The products of these  
363 genes are probably not the only ones responsible for Put or glutamate/aspartate  
364 transport, since *S. meliloti* encodes an additional Put ABC transporter and three  
365 Spd/Put ABC transporters, in addition to numerous amino acid transport systems,  
366 both general and specific [14,26]. The single downstream gene (*smc02982*) in  
367 operon with *odc2* encodes a possible *N*-acetyltransferase that we proposed might  
368 function in the production of *N*-acetylglutamate for Orn and Arg biosynthesis [26,  
369 41]. We found, however, that a *smc02982* null mutant of *S. meliloti* 1021 was an  
370 Arg prototroph that grew normally on MMS [41].

371

372 Cultures of the wild type and mutants were grown in MMS and their ability to  
373 decarboxylate Orn was determined. In comparison to the wild type, the ODC  
374 activities of the Rm8530 *odc1*, *odc2* and *odc1 odc2* mutants were decreased by  
375 14, 55 and 75 %, respectively (Fig. 2). We conclude that it is much more likely that  
376 these reductions in ODC activity result from the inactivation of *odc1* and/or *odc2*  
377 rather than of downstream genes in their operons. From these results we estimate  
378 that all but about 25 % of the total ODC activity in strain Rm8530 is due to the  
379 combined activities of the ODC1 and ODC2, with the latter enzyme accounting for  
380 about 80 % of this. The remaining ODC activity in the double mutant could result  
381 from the predicted ADC (SMa0682) being able to decarboxylate Orn in addition to  
382 or instead of Arg, or by the conversion of the <sup>14</sup>C-Orn assay substrate to <sup>14</sup>C-Arg by  
383 enzymes of the Arg biosynthesis pathway [27], with subsequent decarboxylation of  
384 the <sup>14</sup>C-Arg by the ADC.

385

386 The wild type and mutant strains were grown in MMS under control (non-stress) or  
387 abiotic stress conditions to determine how inactivating the decarboxylases affected  
388 growth and PA production (Fig. 3). Estimations of relative changes in PA levels  
389 were made by densitometry of DNS-PA spots on HPTLC plates from at least two  
390 independent experiments. Specific growth rates (generations h<sup>-1</sup>) for selected  
391 cultures are shown in Fig. 4. The growth of the mutant strains in PY rich medium  
392 was indistinguishable from that of the wild type (results not shown).

393

394 In wild type Rm8530 grown under control conditions, HSpd, Spd and Put account  
395 for virtually all of the DNS-PAs detected by HPTLC (Fig. 3(d)): relative to this total  
396 quantity set at 1.0, the proportions comprised by each of the three polyamines are  
397 0.31, 0.56 and 0.13, respectively. During growth under the control, saline or acidic  
398 conditions, the *odc1* mutant grew similarly to the wild type (Fig. 3 (a) - (c)) and its  
399 content of HSpd, Spd and Put differed from the wild type by less than 10 %. In  
400 contrast, the *odc2* single and *odc1 odc2* double mutants grew about 40 % slower  
401 than the wild type or the *odc1* mutant (Fig. 4) and reached a lower cell yield under  
402 all conditions, most notably with acid stress (Fig. 3(a)-(c)). In the rhizobial plant

403 pathogen *Agrobacterium tumefaciens* strain C58, an *odc* deletion mutant produced  
404 much less Put and Spd and grew more slowly than the wild type in minimal  
405 medium [25]. The *A. tumefaciens* ODC and the *S. meliloti* ODC2 share over 90 %  
406 deduced amino acid sequence identity and may thus fulfill similar physiological  
407 functions.

408

409 In the wild type under saline stress (Fig. 3(d)), HSpd was undetectable and Put  
410 decreased by > 90 %, but Spd levels were maintained at a high level similar to that  
411 seen under control conditions. HSpd levels decrease in salt-stressed  
412 *Sinorhizobium fredii* P220 (a relatively salt- and acid-resistant strain), where it was  
413 proposed that having less of this polycation offsets the increase in positive charges  
414 caused by the rise in cytosolic K<sup>+</sup> that occurs under these conditions [18]. With  
415 acidic stress, wild type Rm8530 had a nearly 4-fold decrease in Put, while HSpd  
416 and Spd levels remained constant. In *S. fredii* P220 HSpd levels increase 2-fold  
417 at pH 4 as compared to pH 9.5, which is an acidic stress much more drastic than  
418 the pH 5.5 versus pH 6.8 stress that we imposed on *S. meliloti* in our experiments.  
419 Under acidic conditions, HSpd may provide cytosolic buffering or protect  
420 macromolecules from acid denaturation [18].

421

422 PA levels in the *odc1* mutant differed by no more than 10 % from the wild type  
423 under all of the growth conditions tested. The *odc2* mutant grown under control  
424 conditions lacked detectable Put and produced 9 and 18 % the wild type levels of  
425 HSpd and Spd, respectively. It also contained some apparent NSpd in the free  
426 fraction that accounted for 4.3 % of the total PAs. The PA profile of the *odc1 odc2*  
427 double mutant from control cultures was similar to that of the *odc2* single mutant  
428 (including the presence of free NSpd), except that Put was present at 11 % of the  
429 wild type level. The reduction in growth caused by the inactivation of the *S. meliloti*  
430 *odc2* is similar to what occurs in *R. leguminosarum* and *A. tumefaciens* when Put  
431 synthesis is lowered by treatment with the ODC inhibitor dimethylfluoroornithine or  
432 by inactivation of the *odc* gene, respectively [23,25]. In both the *odc2* and double

433 mutants, the levels of Put, Spd and HSpd were also markedly lower than in the wild  
434 type during growth under salt or acid stress (Fig. 3 (d)).

#### 435 **Chemical complementation restores growth and PA levels in the *odc2* mutant**

436 Testing the ability of an exogenous PA to restore the normal phenotype of a PA  
437 mutant is called chemical complementation [9,11,23,24]. The effect of chemical  
438 complementation on the specific growth rate ( $\mu$ , or generations  $h^{-1}$ ; Fig. 4) and PA  
439 content (Fig. 5) of the Rm8530 wild type and selected PA mutants was determined  
440 under control, salt stress and acid stress conditions. For these experiments, we  
441 used exogenous Put and Spd for chemical complementation since these PAs  
442 result directly or indirectly from Orn decarboxylation (Fig. 1). HSpd is derived  
443 directly from Put but was not tested because it is not commercially available. NSpd  
444 was used for chemical complementation since its synthesis does not require Put  
445 (Fig. 1).

446

447 In control (non-stressed) cultures without added PAs,  $\mu$  values of the *odc1*, *odc2*  
448 and *odc1 odc2* mutants were 93, 59 and 60 % that of the wild type (Fig. 4(a)). The  
449 specific growth rate of the *odc1* mutant grown under stress or non-stress  
450 conditions with or without exogenous PAs differed from the wild type by no more  
451 than 13 %, in contrast to the much more pronounced growth defects found in the  
452 *odc2* and *odc1 odc2* mutants. As mentioned, the levels of Put, HSpd and Spd in  
453 the *odc1* mutant are comparable to those of the wild type, while they are similarly  
454 and drastically reduced to low levels in the *odc2* and double mutants (Fig. 3(d)). In  
455 cultures without added PAs, growth under salt and acidic stress reduced the  $\mu$  of  
456 Rm8530 by 21 and 27 %, respectively, in comparison to non-stress conditions (Fig.  
457 4). Under salt stress conditions, the  $\mu$  values of the mutants were less affected  
458 relative to the wild type grown under the same condition, with the *odc1*, *odc2* and  
459 double mutants having 102, 86 and 85 % wild type growth rates (Fig. 4(b)). This  
460 may occur because *S. meliloti* responds to salt stress by lowering its total PA  
461 content (Fig. 3(d)), and so the *odc2* and double mutants, with their very low PA  
462 levels, are less affected for growth under saline conditions than under control  
463 conditions. Under acid stress, the *odc1*, *odc2* and double mutants had  $\mu$  values of



464 105, 57 and 55 % of wild type (Fig. 4(c)). Thus, under this stress condition, the  
465 lack of ODC1 activity has essentially no effect on growth, while the mutants lacking  
466 ODC2 activity have growth reductions similar to that found under control  
467 conditions.

468

469 For wild type Rm8530 grown under control (non-stress) conditions (Fig. 4(a)),  
470 exogenous Put or Spd caused a reduction in  $\mu$  of 8-9 % and NSpd caused a 21 %  
471 decrease. Lesser decreases in wild type  $\mu$  values were caused by the PAs under  
472 salt stress (reductions of 4, 6 and 12 % for Put, Spd and NSpd, respectively).  
473 Under acid stress, wild type  $\mu$  values decreased 7 % with Put, increased 1.1 fold  
474 with Spd and were unchanged with NSpd. For the *odc2* and double mutant grown  
475 under stress or non-stress conditions, Put supplementation restored  $\mu$  to 94 to 96  
476 % that of wild type. When these mutants were grown under control or salt stress  
477 conditions, exogenous Spd restored growth rates to 89-96 % that of wild type,  
478 while under acid stress it allowed growth at slightly higher than wild type  $\mu$  values  
479 (Fig. 4). When grown in NSpd-supplemented cultures under non-stress conditions,  
480 the growth of the *odc2* and double mutants were restored to only 66 and 69 % that  
481 of wild type, respectively. Under salt and acid stress, these values ranged from 79-  
482 89 % of wild type. Thus, exogenous NSpd was not as effective as Put or Spd in  
483 restoring the growth of *odc2* and double mutants under any growth condition. It is  
484 interesting to note that the growth restoration caused with NSpd was greater under  
485 stress than non-stress conditions.

486

487 Under control conditions, Rm8530 cells from cultures grown with 1 mM Put (Fig.  
488 5(a)) had 77 % less Put, 30 % less Spd and 1.9-fold more HSpd relative to cells  
489 grown without added Put (Fig. 3(d) and results not shown). Cells from the Put-  
490 supplemented cultures also contained a trace of DAP, which accounted for than 1  
491 % of the total PAs present (Fig. 5(a)). The decrease in Put might result from its  
492 use in HSpd synthesis. DAP is not derived from Put and it is not known whether  
493 Put can modulate the production of PAs in the L-aspartate  $\beta$ -semialdehyde (L-Asp  
494  $\beta$ -SA) branch of the synthesis pathway (Fig. 1).

495 Supplementation of Rm8530 control cultures with Spd caused a modest (13 %)   
496 decrease in intracellular Spd concentration, a 1.6-fold increase in Put and no   
497 change in HSpd, but caused the appearance of detectable DAP (Fig. 3(d) and Fig.   
498 5(b) and results not shown). As described later, the drastic reduction in *odc2*   
499 transcription observed in cells from Spd-supplemented cultures suggests that the   
500 nearly unchanged level of intracellular Spd could result from its reduced synthesis   
501 by ODC2 being offset by the uptake of exogenous Spd. Whether the increase in   
502 Put is derived from the retroconversion of Spd to Put, as occurs in *A. tumefaciens*   
503 [11], is unknown. In Spd-supplemented MMS-salt cultures, HSpd was   
504 undetectable while Put and DAP levels were greatly decreased in comparison to   
505 their levels in the control cultures. Under these conditions, Spd was the only PA   
506 present at high levels. Cultures grown under acidic conditions with added Spd   
507 produced significantly less HSpd and Put than non-stressed cultures, but had the   
508 same or slightly higher levels of DAP. For all of the strains grown under all   
509 conditions, the addition of NSpd to the medium resulted in a high level of its   
510 accumulation, an apparent total absence of Spd and at most trace levels of HSpd   
511 and Put, and remarkably high amounts of DAP (Fig. 5(c)). In *A. tumefaciens*, cells   
512 grown in the presence of NSpd (which is not produced by this organism) also   
513 produce little intracellular Spd [25]. In *S. meliloti*, the intriguing possibility exists   
514 that NSpd has regulatory effects on the production on PAs derived from Put.

515

#### 516 **Genetic complementation restores growth and PA levels in the *odc2* mutant**

517 To confirm that the inactivation of the *odc2* gene was responsible for the altered   
518 phenotype of the *odc2* mutant, we introduced the *odc2* gene into the mutant on   
519 plasmid pBB5-*odc2* (Table 1). The resulting transconjugant, 8530 *odc2*(pBB5-   
520 *odc2*), had its Orn decarboxylating activity restored to nearly that of the wild type,   
521 while the activity in the mutant containing the cloning vector alone (strain 8530   
522 *odc2*(pBB5)) was very similar to that of the uncomplemented mutant (Fig. 2).   
523 Strain 8530 *odc2*(pBB5-*odc2*) also grew similarly to the wild type under stress and   
524 non-stress growth conditions, and its ability to produce PAs was restored to   
525 approximately wild type levels (Fig. 6). These results are consistent with the

526 inactivation of the *odc2* gene being the cause of the growth and PA production  
527 phenotypes of the *odc2* mutant. The *odc2* mutant also produced some apparent  
528 NSpd in the free PA fraction (Fig. 6(d)). In comparison to the uncomplemented  
529 mutant, strain 8530 *odc2*(pBB5) had a slower growth rate under all conditions,  
530 perhaps due to the metabolic burden of plasmid maintenance. As expected, strain  
531 8530 *odc2*(pBB5) produced low levels of PAs similar to the mutant without the  
532 plasmid (Fig. 6).

533

534 Although the introduction of genes for metabolic enzymes cloned on plasmid pBB5  
535 into *S. meliloti* can increase the gene products activity several-fold, presumably  
536 due to increased copy number [27], we did not find increased in ODC activity (Fig.  
537 2) or over-production of PAs (Fig 6(d)) in strain 8530 *odc2*(pBB5-*odc2*).

538

#### 539 **Transcriptional expression of *odc2* under different growth conditions**

540 The expression of  $\beta$ -glucuronidase (*gusA*) transcriptional fusions to the *odc1* and  
541 *odc2* genes was determined in strain Rm8530 grown under different growth  
542 conditions. The *odc1* gene is part of a predicted four gene operon and lacks a  
543 transcriptional start site (TSS) [37]: we found that a *odc1::gusA* fusion produced a  
544 low level of Gus activity (50-115 nmol min<sup>-1</sup> mg protein<sup>-1</sup>). *In vivo*, *odc1*  
545 transcription may be linked to that of the upstream gene (*smc0682*), which is not  
546 part of the fusion construct.

547

548 Under the growth conditions tested, the GUS specific activity from the *odc2::gusA*  
549 fusion changed over a 7-fold range, from about 400 to 2900 nmol min<sup>-1</sup> mg protein<sup>-1</sup>  
550 (Fig. 7). Although *odc2* also lacks a recognizable TSS, it is the first gene in an  
551 apparent two-gene operon [37] and the results described below suggest that *odc2*  
552 expression is modulated in response to growth conditions.

553

554 In comparison to control (non-stress) conditions, *odc2* transcription decreased 69  
555 % under salt stress (Fig. 7), consistent with the 94 % reduction in Put in these cells  
556 (Fig 3(d) and results not shown). The decreased Put content in salt stressed cells

557 is not explained by its conversion to HSpd and/or Spd, since the combined quantity  
558 of these PAs was nearly identical in the control and salt-stressed cells. Decreased  
559 expression of *odc2* was also reported in a transcriptomic study of *S. meliloti* 1021  
560 grown under salt stress [42]. Acidic stress increased *odc2* transcription 1.5-fold,  
561 which does not correlate with the 77 % decrease in Put levels seen during growth  
562 at low pH (Fig. 3(d)).

563

564 Cells grown in cultures supplemented with the exogenous Put precursor amino  
565 acids Arg or Orn expressed *odc2* at a level 20 and 28 % less than in cells from  
566 unsupplemented cultures. Assigning these effects solely to the exogenous amino  
567 acid added to the cultures is complicated by the ability of *S. meliloti* to convert Arg  
568 to Orn using arginase and to metabolize Orn to Arg by activities of the Arg  
569 synthesis pathway [14]). We can tentatively conclude that Orn, the major substrate  
570 for ODC2, does not induce *odc2* expression.

571

572 To determine the effect of exogenous PAs on *odc2* transcription, we used Put and  
573 Spd, which result directly and indirectly from Orn decarboxylation, respectively, and  
574 DAP and NSpd, which are not derived from Put (Fig 1). Exogenous Put, Spd and  
575 NSpd inhibited *odc2* transcription by 58, 79 and 36 % respectively, while DAP  
576 resulted in a small increase in its transcription (Fig. 7). Thus, the PA products  
577 resulting from Orn decarboxylation inhibited *odc2* transcription to a greater degree  
578 than the PAs from the L-Asp  $\beta$ -SA branch of the pathway.

579

580 In summary, we have shown that Put and/or PAs derived from it are required for  
581 the normal growth of *S. meliloti* Rm8530. ODC2 (SMc02983) is a bifunctional  
582 Lys/Orn decarboxylase responsible for synthesizing the majority of Put produced  
583 by strain Rm8530, and changes in *odc2* transcription observed under some growth  
584 conditions are consistent with observed changes in PA levels. The *S. meliloti*  
585 ODC1 (SMa0680) is a monofunctional ODC that contributes a minor portion of the  
586 ODC activity in Rm8530.

587

588 The results presented here provide a basis for further experiments aimed at  
589 deciphering the enzymology and regulation of PA metabolism in *S. meliloti*, which  
590 provides an attractive model system due to its extended PA biosynthetic  
591 capabilities [14]. We are currently addressing some of these questions, along with  
592 determining the physiological roles of specific PAs in free-living and symbiotically-  
593 associated *S. meliloti*.

594

### 595 **Funding information**

596 Work at the UNAM was supported by DGAPA-PAPIIT Grants IN210114 and  
597 IN206317 to M. F. D. The York Centre of Excellence in Mass Spectrometry was  
598 created thanks to a major capital investment through Science City York, supported  
599 by Yorkshire Forward with funds from the Northern Way Initiative, and subsequent  
600 support from EPSRC (EP/K039660/1; EP/M028127/1).

601

### 602 **Acknowledgements**

603 Victor A. Becerra-Rivera is a doctoral student from Programa de Doctorado en  
604 Ciencias Biomédicas, Universidad Nacional Autónoma de México (UNAM) and  
605 received fellowship 574042 from CONACYT. We thank María J. Soto  
606 (Departamento de Microbiología del Suelo y Sistemas Simbióticos de la Estación  
607 Experimental del Zaidín, CSIC, Granada, Spain) for providing *S. meliloti* strain  
608 Rm8530 and Lourdes Girard (CCG-UNAM) for providing the p53lw primer and the  
609 pBBRMCre plasmid.

610

### 611 **Conflict of interest**

612 The authors declare that there are no conflicts of interest.

613

### 614 **References**

- 615 1. Tabor CW, Tabor H. Polyamines. *Annu Rev Biochem* 1984;53:749-790.
- 616 2. Hamana K, Matsuzaki S. Polyamines as a chemotaxonomic marker in bacterial  
617 systematics. *Crit Rev Microbiol* 1992;18:261-283.

- 618 3. Algranati ID. Polyamine metabolism in *Trypanosoma cruzi*: studies on the  
619 expression and regulation of heterologous genes involved in polyamine  
620 biosynthesis. *Amino Acids* 2010;38:645-51.
- 621 4. Miller-Fleming L, Olin-Sandoval V, Campbell K, Ralser M. Remaining mysteries  
622 of molecular biology: The role of polyamines in the cell. *J Mol Biol*  
623 2015;427:3389–3406.
- 624 5. Michael AJ. Polyamines in eukaryotes, bacteria, and archaea. *J Biol Chem*  
625 2016;291:14896-14903.
- 626 6. Soksawatmaekhin W, Kuraishi A, Sakata K, Kashiwagi K, Igarashi K, Excretion  
627 and uptake of cadaverine by CadB and its physiological functions in  
628 *Escherichia coli*. *Mol Microbiol* 2004;51:1401–1412.
- 629 7. Sturgill G, Rather PN. Evidence that putrescine acts as an extracellular signal  
630 required for swarming in *Proteus mirabilis*. *Mol Microbiol* 2004;51:437-446.
- 631 8. Shah P, Swiatlo E. A multifaceted role for polyamines in bacterial pathogens.  
632 *Mol Microbiol* 2008;68:4–16.
- 633 9. Lee J, Sperandio V, Frantz DE, Longgood J, Camilli A *et al*. An alternative  
634 polyamine biosynthetic pathway is widespread in bacteria and essential for  
635 biofilm formation in *Vibrio cholerae*. *J Biol Chem* 2009;284:9899-907.
- 636 10. Cockerell SR, Rutkovsky AC, Zayner JP, Cooper RE, Porter LR *et al*. *Vibrio*  
637 *cholerae* NspS, a homologue of ABC-type periplasmic solute binding  
638 proteins, facilitates transduction of polyamine signals independent of their  
639 transport. *Microbiology* 2014;160:832-843.
- 640 11. Kim SH, Wang Y, Khomutov M, Khomutov A, Fuqua C, Michael AJ. The  
641 essential role of spermidine in growth of *Agrobacterium tumefaciens* is  
642 determined by the 1,3-diaminopropane moiety. *ACS Chem Biol*  
643 2016;11:491-9.
- 644 12. López-Gómez M, Hidalgo-Castellanos J, Lluch C, Herrera-Cervera JA.  
645 Epibrassinolide ameliorates salt stress effects in the symbiosis *Medicago*  
646 *truncatula*-*Sinorhizobium meliloti* and regulates the nodulation in cross-talk  
647 with polyamines. *Plant Physiol Biochem* 2016;108:212-221.

- 648 13. Lucas PM. Ornithine and lysine decarboxylation in bacteria. In: D'Mello FJ  
649 (editor) *Handbook of Microbial Metabolism of Amino Acids*. Wallingford,  
650 Oxfordshire: CAB International; 2017. pp. 116-127.
- 651 14. Dunn MF. Rhizobial Amino Acid Metabolism: Polyamine Biosynthesis and  
652 Functions. In: D'Mello FJ (editor) *Handbook of Microbial Metabolism of*  
653 *Amino Acids*. Wallingford, Oxfordshire: CAB International; 2017. pp. 352-  
654 370.
- 655 15. Hamana K, Minamisawa K, Matsuzaki S. Polyamines in *Rhizobium*,  
656 *Bradyrhizobium*, *Azorhizobium* and *Agrobacterium*. *FEMS Microbiol Lett*  
657 1990;71: 71-76.
- 658 16. Hamana K, Sakamoto A, Tachiyanagi S, Terauchi E, Takeuchi M. Polyamine  
659 profiles of some members of the alpha subclass of the class Proteobacteria:  
660 Polyamine analysis of twenty recently described genera. *Microbiol Cult Coll*  
661 2003;19:13-21.
- 662 17. Vassileva V, Ignatov, G. Polyamine-induced changes in symbiotic parameters  
663 of the *Galega orientalis-Rhizobium galegae* nitrogen-fixing system. *Plant*  
664 *Soil* 1999;210:83-91.
- 665 18. Fujihara S, Yoneyama T. Effects of pH and osmotic stress on cellular  
666 polyamine contents in the soybean rhizobia *Rhizobium fredii* P220 and  
667 *Bradyrhizobium japonicum* A1017. *Appl Environ Microbiol* 1993;59:1104-  
668 1109.
- 669 19. López-Gómez M, Hidalgo-Castellanos J, Iribarne C, Lluch C. Proline  
670 accumulation has prevalence over polyamines in nodules of *Medicago*  
671 *sativa* in symbiosis with *Sinorhizobium meliloti* during the initial response to  
672 salinity. *Plant Soil* 2014;374: 149-159.
- 673 20. Palma F, López-Gómez M Tejera NA, Lluch C. Involvement of abscisic acid in  
674 the response of *Medicago sativa* plants in symbiosis with *Sinorhizobium*  
675 *meliloti* to salinity. *Plant Sci* 2014;223:16-24.
- 676 21. López-Gómez M, Hidalgo-Castellanos J, Muñoz-Sánchez JR, Marín-Peña AJ,  
677 Lluch C, Herrera-Cerver, JA. Polyamines contribute to salinity tolerance in

- 678 the symbiosis *Medicago truncatula*-*Sinorhizobium meliloti* by preventing  
679 oxidative damage. *Plant Physiol Biochem* 2017;116:9-17.
- 680 22. Braeken K, Daniels R, Vos K, Fauvart M, Debkumari Bachaspatimayum D,  
681 Vanderleyden J, Michiels J. Genetic determinants of swarming in *Rhizobium*  
682 *etli*. *Microbial Ecol* 2008;55:54-64.
- 683 23. Shaw FL. *From prediction to function: Polyamine biosynthesis and formate*  
684 *metabolism in the  $\alpha$ - and  $\epsilon$ -Proteobacteria*. Ph.D Thesis. England: Institute  
685 of Food Research, Norwich Research Park; 2011.
- 686 24. López-Gómez M, Cobos-Porras L, Prell J, Lluch C. Homospermidine synthase  
687 contributes to salt tolerance in free-living *Rhizobium tropici* and in symbiosis  
688 with *Phaseolus vulgaris*. *Plant Soil* 2016;404:413–425.
- 689 25. Wang Y, Kim SH, Natarajan R, Heindl JE, Brugerm EL *et al*. Spermidine  
690 inversely influences surface interactions and planktonic growth in  
691 *Agrobacterium tumefaciens*. *J Bacteriol* 2016;198:2682-2691.
- 692 26. Dunn MF. Key roles of microsymbiont amino acid metabolism in rhizobia-  
693 legume interactions. *Crit Rev Microbiol* 2015;41:411-451.
- 694 27. Hernández VM, Girard L, Hernández-Lucas I, Vázquez A, Ortiz-Ortiz C *et al*.  
695 Genetic and biochemical characterization of arginine biosynthesis in  
696 *Sinorhizobium meliloti* 1021. *Microbiology* 2015;161:1671-1682.
- 697 28. Dunn MF, Araíza G, Cevallos MA, Mora J. Regulation of pyruvate carboxylase  
698 in *Rhizobium etli*. *FEMS Microbiol Lett* 1997;157:301-306.
- 699 29. Sambrook J, Fritsch EF, Maniatis T. *Molecular Cloning: A Laboratory Manual*  
700 New York: Cold Spring Harbor Laboratory Press; 1989.
- 701 30. Landeta C, Dávalos A, Cevallos MA, Geiger O, Brom S, Romero D. Plasmids  
702 with a chromosome-like role in Rhizobia. *J Bacteriol* 2011;193:1317-1326.
- 703 31. Romano A, Trip H, Lolkema JS, Lucas PM. Three-component lysine/ornithine  
704 decarboxylation system in *Lactobacillus saerimneri* 30a. *J Bacteriol*  
705 2013;195:1248-1254.
- 706 32. Girard L, Brom S, Dávalos A, López O, Soberón M, Romero, D. Differential  
707 regulation of *fixN*-reiterated genes in *Rhizobium etli* by a novel *fixL*-*fixK*  
708 cascade. *Mol Plant-Microbe Interact* 2000;13:1283-1292.



- 709 33. Goldschmidt MC, Lockhart BM. Rapid methods for determining decarboxylase  
710 activity: arginine decarboxylase. *Appl Microbiol* 1971;22:350-357.
- 711 34. Ngo TT, Brillhart KL, Davis RH, Wong RC, Bovaird JH *et al.*  
712 Spectrophotometric assay for ornithine decarboxylase. *Anal Biochem*  
713 1987;160:290-293.
- 714 35. Phan APH, Ngo TT, Lenhoff HM. Spectrophotometric assay for lysine  
715 decarboxylase. *Anal Biochem* 1982;120:193-197.
- 716 36. Bradford MM. A rapid and sensitive method for the quantitation of microgram  
717 quantities of protein utilizing the principle of protein-dye binding. *Anal*  
718 *Biochem* 1976;72:248-254.
- 719 37. Schlüter JP, Reinkensmeier J, Barnett MJ, Lang C, Krol E, Giegerich R, *et al.*  
720 Global mapping of transcription start sites and promoter motifs in the  
721 symbiotic  $\alpha$ -proteobacterium *Sinorhizobium meliloti* 1021. *BMC Genomics*  
722 2013;14:156.
- 723 38. Slocum RD, Flores HE, Galston AW, Weinstein LH. Improved method for  
724 HPLC analysis of polyamines, agmatine and aromatic monoamines in plant  
725 tissue. *Plant Physiol* 1989;89:512-517.
- 726 39. Pedrol N, Tiburcio AF. Polyamines determination by TLC and HPLC. In: Roger  
727 MJR (editor). *Handbook of Plant Ecophysiology Techniques*. The  
728 Netherlands: Kluwer Academic Publishers; 2001. pp. 335–363.
- 729 40. Pellock BJ, Teplitski M, Boinay RP, Bauer WD, Walker GC. A LuxR homolog  
730 controls production of symbiotically active extracellular polysaccharide II by  
731 *Sinorhizobium meliloti*. *J Bacteriol* 2002;184:5067-5076.
- 732 41. Paulino, EM. Búsqueda del gen que codifica para la enzima *N*-acetilglutamato  
733 sintasa por mutagénesis. Bachelors Thesis. Mexico: Universidad Autónoma  
734 del Estado de Morelos; 2013.
- 735 42. Domínguez-Ferreras A, Pérez-Arnedo R, Becker A, Olivares J, Soto MJ,  
736 Sanjuán J. Transcriptome profiling reveals the importance of plasmid  
737 pSymB for osmoadaptation of *Sinorhizobium meliloti*. *J Bacteriol*  
738 2006;188:7617-7625.

- 739 43. Kovach ME, Elzer PH, Hill DS, Robertson GT, Farris MA *et al.* Four new  
740 derivatives of the broad-host-range cloning vector pBBR1MCS, carrying  
741 different antibiotic-resistance cassettes. *Gene* 1995;160:175-176.
- 742 44. Schäfer A, Tauch A, Jäger W, Kalinowski J, Thierbach G, Pühler A. Small  
743 mobilizable multi-purpose cloning vectors derived from the *Escherichia coli*  
744 plasmids pK18 and pK19: selection of defined deletions in the chromosome  
745 of *Corynebacterium glutamicum*. *Gene* 1994;145:69-73.
- 746 45. Martínez-Salazar JM, Romero D. Role of *ruvB* gene in homologous  
747 recombination in *Rhizobium etli*. *Gene* 2000;243:125-131.
- 748 46. Figurski DH, Helinski DR. Replication of an origin-containing derivative of  
749 plasmid RK2 dependent on a plasmid function provided in trans. *Proc Natl*  
750 *Acad Sci (USA)* 1979;76:1648-1652.

751

752

753

754

755

756

757

758 **Table 1.** Strains and plasmids used in this study.

759

Strain or plasmid	Relevant characteristics	Source or reference
<b><i>E. coli</i> strains</b>		
BL21(DE3)	Strain for protein expression	Invitrogen
DH5 $\alpha$	Cloning strain	Laboratory collection
JM109	Cloning strain	Laboratory collection
<b><i>S. meliloti</i> strains</b>		
Rm8530	<i>S. meliloti</i> 1021 <i>expR</i> <sup>+</sup> , Sm <sup>r</sup>	M. Soto, Estación Experimental del Zaidín, CSIC, Granada, Spain
8530 <i>odc1</i>	Rm8530 <i>sma0680::loxP</i> Sp <i>odc1</i> null mutant, Sm <sup>r</sup> Sp <sup>r</sup>	This study
8530 <i>odc2</i>	Rm8530 <i>smc02983::loxP</i> Sp <i>odc2</i> null mutant, Sm <sup>r</sup> Sp <sup>r</sup>	This study
8530 <i>odc1 odc2</i>	Rm8530 <i>sma0680::loxP smc02983::loxP</i> Sp <i>odc1 odc2</i> null double mutant, Sm <sup>r</sup> Sp <sup>r</sup>	This study
8530 <i>odc2</i> (pBB5)	Rm8530 <i>smc02983::loxP</i> Sp <i>odc2</i> null mutant containing plasmid pBB5, Sm <sup>r</sup> Sp <sup>r</sup> Gm <sup>r</sup>	This study
8530 <i>odc2</i> (pBB5- <i>odc2</i> )	Rm8530 <i>smc02983::loxP</i> Sp <i>odc2</i> null mutant complemented with the <i>odc2</i> gene <i>in trans</i> , Sm <sup>r</sup> Sp <sup>r</sup> Gm <sup>r</sup>	This study
<b>Plasmids</b>		
pBB5	Broad-host-range vector pBBR1MCS-5, Gm <sup>r</sup>	[43]
pBB5- <i>odc2</i>	pBBR1MCS-5 containing <i>smc02983</i> with native promoter and terminator regions, Gm <sup>r</sup>	This study
pBBMCS-53	$\Delta$ <i>placZ</i> pBBR1MCS-5 derivative	[32]

	with promoterless <i>gusA</i> , Km <sup>r</sup>	
pBB53odc1:: <i>gusA</i>	Transcriptional <i>sma0680</i> :: <i>gusA</i> fusion in pBBMCS-53	This study
pBB53odc2:: <i>gusA</i>	Transcriptional <i>smc02983</i> :: <i>gusA</i> fusion in pBBMCS-53	This study
pCRodc1	Rm8530 genome region containing <i>odc1</i> cloned in pTopo	This study
pCRodc2	Rm8530 genome region containing <i>odc2</i> cloned in pTopo	This study
pKodc1	Rm8530 genome region containing <i>odc1</i> cloned in pK18mobsacB	This study
pKodc2	Rm8530 genome region containing <i>odc2</i> cloned in pK18mobsacB	This study
pK18mobsacB	Broad-host range gene replacement vector, Km <sup>r</sup>	[44]
pKodc1:: <i>loxSp</i>	<i>odc1</i> :: <i>loxP</i> Sp fragment cloned in pK18mobsacB	This study
pKodc2:: <i>loxSp</i>	<i>odc2</i> :: <i>loxP</i> Sp fragment cloned in pK18mobsacB	This study
pMS102 <i>loxSp</i> 17	Source of the <i>loxP</i> Sp interposon, Sp <sup>r</sup>	[45]
pRK2013	Helper plasmid, Km <sup>r</sup>	[46]
pET-Sumo	Expression vector for production of 6His-Sumo-tagged proteins, Km <sup>r</sup>	Invitrogen
pSumo-odc1	pET-Sumo containing the cloned Rm8530 <i>odc1</i> gene	This study
pSumo-odc2	pET-Sumo containing the cloned Rm8530 <i>odc2</i> gene	This study
pTopo	pCR2.1Topo vector for cloning PCR products, Km <sup>r</sup>	Invitrogen
pTZ57R/T	InstAclone vector for cloning PCR	Thermo

products, Ap<sup>r</sup> (Cb<sup>r</sup>)

pBBRMCre

Plasmid used for deleting the loxP [30]

Sp interposon inserted in *smc0680*

760

761

762

763

764 **FIGURE LEGENDS**

765

766 **Fig. 1.** Predicted polyamine synthesis pathways in *S. meliloti* Rm8530.  
767 Abbreviations not described in the text:  $\alpha$ -KG,  $\alpha$ -ketoglutarate; CNSpd,  
768 carboxynorspermidine; CANSDC, CNSpd decarboxylase; CANSDH, CNSpd  
769 dehydrogenase; CSpd; carboxyspermidine; DABA, diaminobutyric acid; DABA AT,  
770 DABA aminotransferase; DABA DC, DABA decarboxylase; L-Glu, L-glutamate;  
771 HSS, homospermidine synthase. Modified from [14].

772

773 **Fig. 2.** Specific activities of Orn decarboxylation by *S. meliloti* strains grown in  
774 MMS, normalized to that of the Rm8530 wild type (100 % = 3968 U). Values are  
775 the mean  $\pm$  SD for two independent experiments. Values for columns marked with  
776 the same letter are not statistically different according to a t-student test.

777

778 **Fig. 3.** Growth and PA content of *S. meliloti* cultured under non-stress and stress  
779 conditions. Panels (a), (b) and (c) represent culture growth under control, salt  
780 stress and acidic stress conditions, respectively. Strains and line colors: Rm8530  
781 wild type, black; 8530 *odc1*, pink; 8530 *odc2*, green; 8530 *odc1 odc2*, blue. Panel  
782 (d) shows HPTLC detection of dansyl-PAs from 32 h cultures. Lane S contains  
783 dansyl-PA standards with their identities shown at the right side of the first plate  
784 image. *S. meliloti* dansyl-PA samples are: Lane 1, Rm8530; Lane 2, 8530 *odc1*;  
785 Lane 3, 8530 *odc2*; Lane 4, 8530 *odc1 odc2*.

786

787 **Fig 4.** Specific growth rates ( $\mu$ , generations  $h^{-1}$ ) of selected *S. meliloti* strains  
788 grown in MMS with or without chemical complementation with exogenous PAs.  
789 Panel (a), control conditions; panel (b), MMS-salt; panel (c), MMS-acid. The PA  
790 added to the cultures is indicated at the bottom of the figure. Bar colors represent:  
791 Rm8530 wild type, blue; 8530 *odc1*, orange; 8530 *odc2*, grey; 8530 *odc1 odc2*,  
792 yellow. Values are normalized to  $\mu$  values of the wild type grown under the three  
793 conditions in media lacking added PAs, where 100 % corresponds to  $\mu$  values of

794 0.179, 0.141 and 0.130 for the MMS, MMS-salt and MMS-acid cultures. Results  
795 are the mean  $\pm$  SD for 2 independent experiments.

796

797 **Fig. 5.** Effect of chemical complementation with exogenous PAs on PA production  
798 by *S. meliloti* strains. HPTLC detection of dansyl-PAs from 32 h cultures. Lane S  
799 contains dansyl-PA standards with their identities shown at the left side of the  
800 plates. Panel (a), MMS plus 1 mM Put; panel (b), MMS plus 1 mM Spd; panel (c),  
801 MMS plus 1 mM NSpd. Lane assignments for all plates: Lane 1, Rm8530 wild type;  
802 Lane 2, 8530 *odc1*; Lane 3, 8530 *odc2*; Lane 4, 8530 *odc1 odc2*.

803

804 **Fig. 6.** Growth and PA content of the genetically complemented 8530 *odc2* mutant.  
805 Panels (a), (b) and (c) show culture growth under control, salt stress and acidic  
806 stress conditions, respectively. Strains and line colors: Rm8530 wild type, black;  
807 8530 *odc2*, green; 8530 *odc2*(pBB5-*odc2*), red; 8530 *odc2*(pBB5), purple. Panel  
808 (d) shows HPTLC detection of dansyl-PAs from 32 h cultures. Lane S contains  
809 dansyl-PA standards with their identities shown at the left side of the plate. *S.*  
810 *meliloti* dansyl-PA samples are: Lane 1, Rm8530; Lane 2, 8530 *odc2*; Lane 3,  
811 8530 *odc2*(pBB5); Lane 4, 8530 *odc2*(pBB5-*odc2*).

812

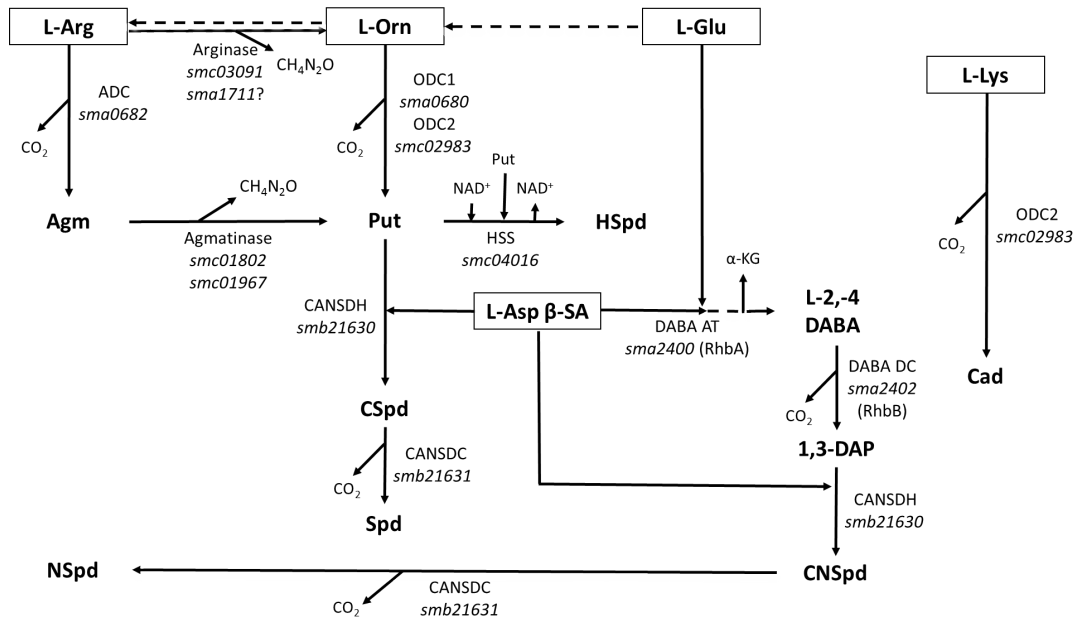
813 **Fig. 7.**  $\beta$ -glucuronidase (Gus) activities produced by *S. meliloti* Rm8530 containing  
814 the *odc2::gusA* transcriptional fusion plasmid. Cells were grown in the indicated  
815 media for 16 h. Values are the mean  $\pm$  SD for two independent experiments, each  
816 with 2 technical replicates of two biological replicates. 1 U = nmol product min<sup>-1</sup> mg  
817 protein<sup>-1</sup>.

818

819

820

821



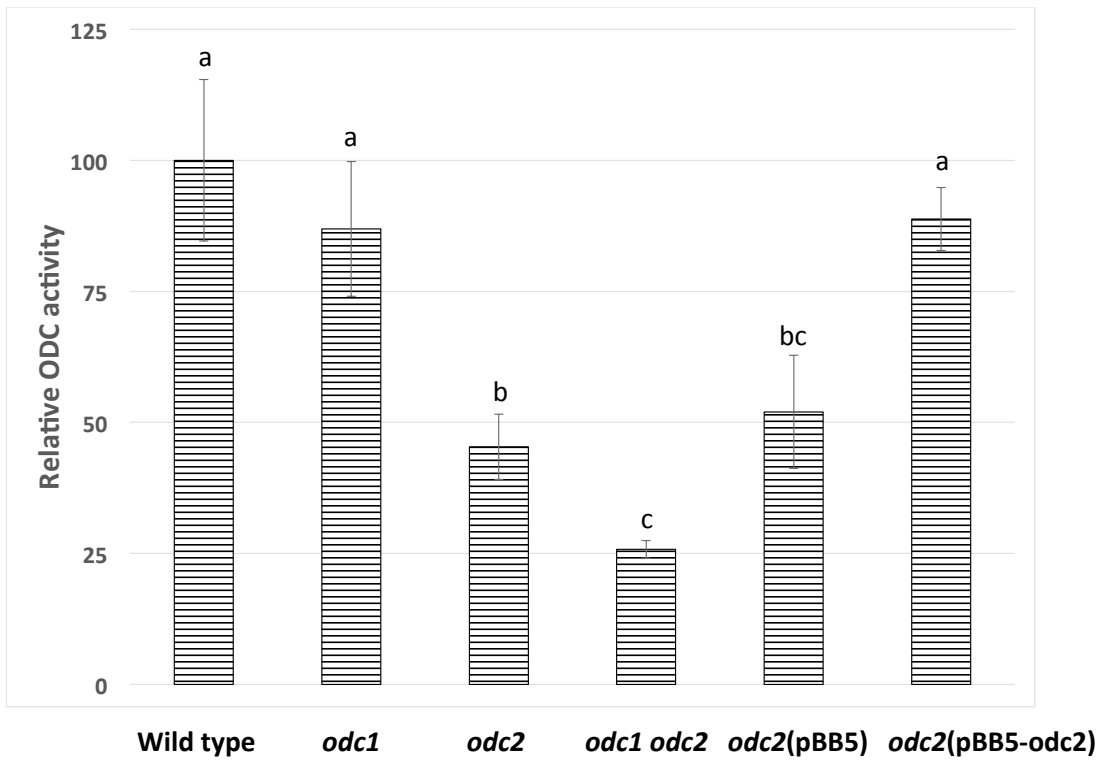
822

823 Fig. 1

824

825



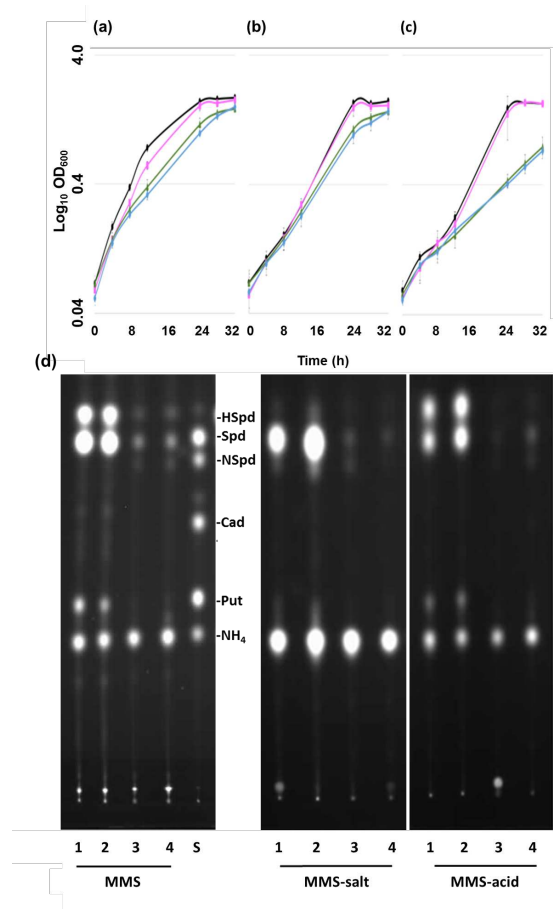


826

827

828 Fig. 2

829



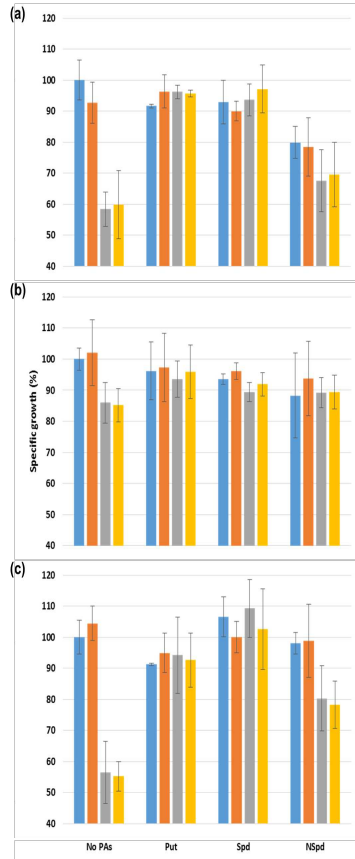
830

831

832

833

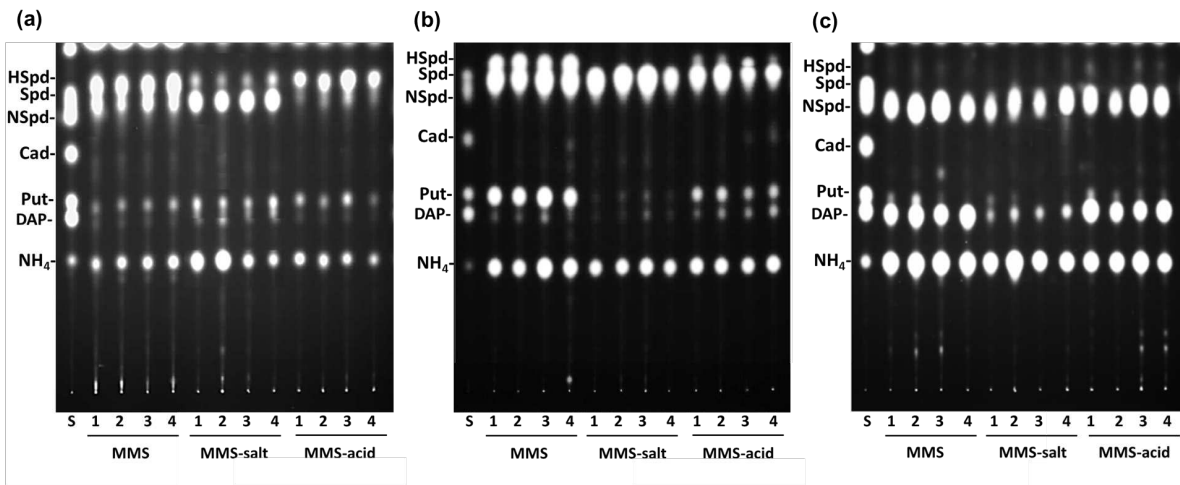
834 Fig. 3



835  
836 Fig. 4

837

838



839

840

841

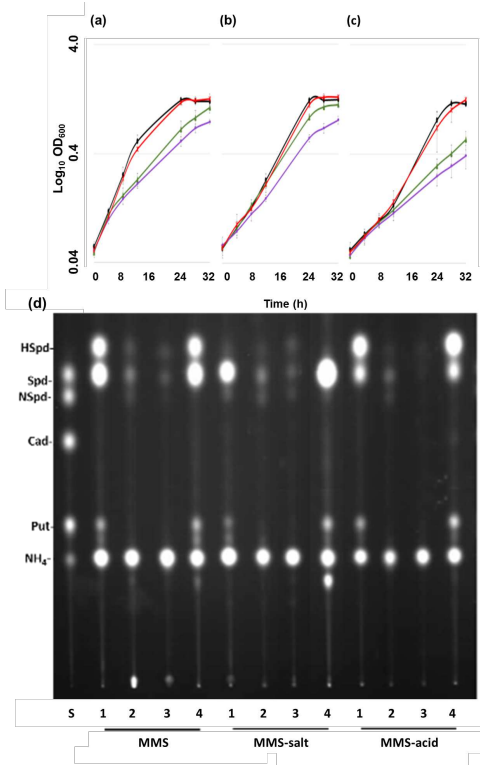
842

843

844

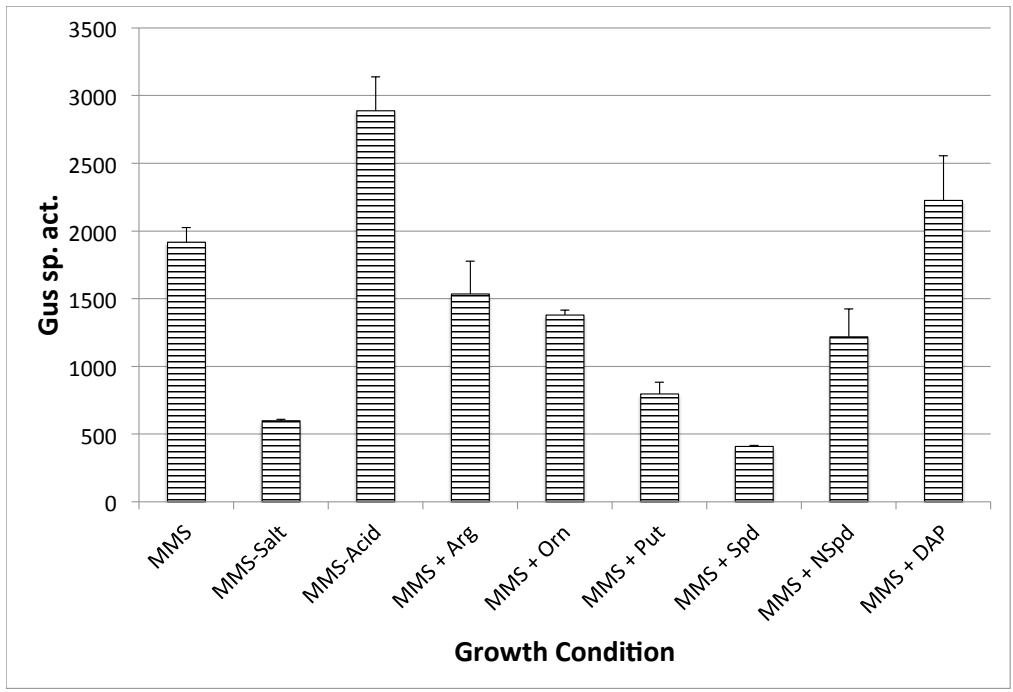
845 Fig. 5

846



847 Fig. 6  
 848

849



850

851

852 Fig. 7

853

854 **Supplementary material**855 **Table S1.** Oligonucleotide primers used in this study.

<b>Primer name</b>	<b>5'-3' nucleotide sequence</b>	<b>Description</b>
Sumo0680F	GTGAAGGCTCCGACCGTC	Forward primer for amplifying the insert used in making pSumo-odc1 and pCR-odc1
Sumo0680R	GATTACTCGCGCACGGCG	Reverse primer for amplifying the insert used in making pSumo-odc1 and pCR-odc1
Sumo02983F	ATGGCCATGACCACCGC	Forward primer for amplifying the insert used in making pSumo-odc2
Sumo02983R	GGATCAGATGACATAGGCC	Reverse primer for amplifying the insert used in making pSumo-odc2
F-02983	TTG GCA CGC ACG AGATCG	Forward primer for amplifying the insert used in making pCR-odc2
R-02983	GGATCAGATGACATAGGCC	Reverse primer for amplifying the insert used in making pCR-odc2
0680gusF	CTACAACCGCCTGGTCAAG	Forward primer used in construction of pBB53odc1::gusA
0680gusR	TCCCAATATAGGCACCAACC	Reverse primer used in construction of pBB53odc1::gusA
02983gusF	GGATGCGGGTCAAGGTATC	Forward primer used in construction of pBB53odc2::gusA
02983gusR	TTGATGGTGTGCCATAGGA	Reverse primer used in construction of pBB53odc2::gusA
p53lw	ACAGGACGTAACATAAGGGAC T	Reverse primer for the <i>gusA</i> gene

856

## 857 **Supplementary Material Figure Legend**

858

859 **Fig. S1.** Analysis of PAs by mass spectrometry. As described in Methods, dansyl-  
860 PAs were prepared from authentic standards or isolated from *S. meliloti* cells,  
861 separated by HPTLC, eluted from the silica gel plates and characterized by matrix-  
862 assisted laser desorption/ionisation (MALDI) high resolution, high mass accuracy  
863 FT-ICR mass spectrometry (MS) and product ion tandem mass spectrometry  
864 (MS/MS). The fragmentation diagrams and product ion spectra used in the  
865 identification of the dansyl-PAs are presented in this figure. Panel (a), resolution  
866 by HPTLC of dansyl-PA standards and unknown bound (spots B1 and B2) or free  
867 (spots F1 through F3) PAs obtained from *S. meliloti* cells. Panel (b), structure of  
868 the dansyl (DNS) chemical group. Panel (c), fragmentation diagram of DNS-Put.  
869 Panel (d), product ion spectrum of DNS-Put standard. Standard Put (two amine  
870 groups, so acquires two DNS groups; Fig. S1(c)) gave an intense signal for its  
871 molecular species at  $m/z$  555.20936 on MALDI FT-ICR mass spectrometry,  
872 corresponding to an elemental composition  $C_{28}H_{35}N_4O_4S_2$  ( $M+H^+$  for (dansyl)<sub>2</sub>Put;  
873 0.1 ppm mass error) and a pattern of isotopic signals matching in relative  
874 intensities very closely those predicted for this molecular composition. CID-MS-MS  
875 of the ion at  $m/z$  555 yielded a product ion spectrum consistent with (dansyl)<sub>2</sub>Put  
876 (Fig. S1(d)). The product ion at  $m/z$  220 is related to that at  $m/z$  234, by loss of one  
877 O atom with transfer of two H atoms. Component F1 migrated similarly to standard  
878 DNS-Put (Fig S1(a)). A strong signal was observed at  $m/z$  555.20921 ( $M+H^+$  for  
879 (DNS)<sub>2</sub>Put; 0.4 ppm mass error), and the product ion spectrum is (Fig. S1(e))  
880 indistinguishable from that obtained from the authentic standard DNS-Put (Fig.  
881 S1(d)), demonstrating that component F1 is Put. Panel (e), product ion spectrum  
882 of spot F1 (see panel (a)), identified as DNS-Put. Panel (f), fragmentation diagram  
883 of DNS-Spd. Panel (g), product ion spectrum of DNS-Spd standard. Standard Spd  
884 (adds three dansyl groups; Fig. S1(f)) gave an intense  $M+H^+$  signal at  $m/z$   
885 845.31810 ( $C_{43}H_{53}N_6O_6S_3$ ; 0.2 ppm mass error), and a pattern of isotopic signals  
886 that match very closely those predicted for a molecule with this composition. CID-  
887 MS-MS of the ion at  $m/z$  845 yielded a product ion spectrum consistent with



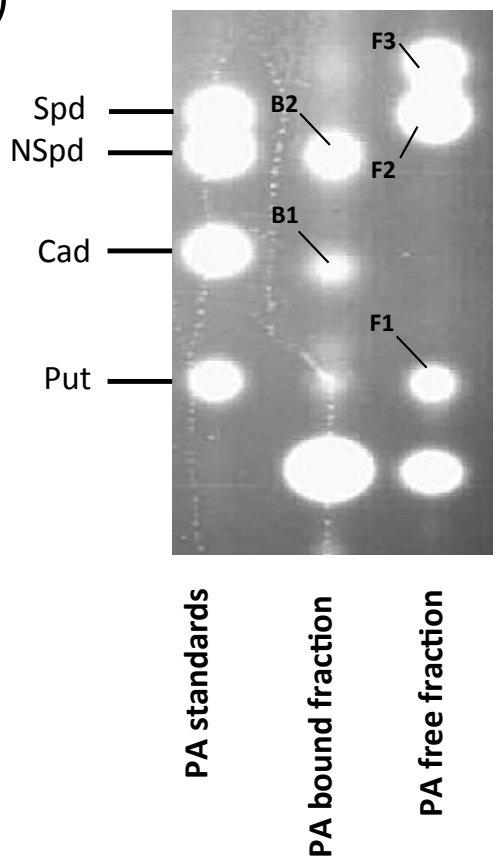
888 (dansyl)<sub>3</sub>Spd (Fig. S1(g)). Component F2 migrated with the DNS-Spd standard  
889 (Fig. S1(a)). A very strong signal was observed at  $m/z$  845.31794 ( $M+H^+$  for  
890 (DNS)<sub>3</sub>Spd; 0.5 ppm mass error), and the product ion spectrum (Fig. S1(h)) is very  
891 similar to that from standard DNS-Spd (Fig. S1(g)), identifying the component as  
892 DNS-Spd (Fig. S1(h)). Panel (h), product ion spectrum of spot F2 (see panel (a)),  
893 identified as DNS-Spd. Panel (i), fragmentation diagram of DNS-NSpd. Panel (j),  
894 product ion spectrum of DNS-NSpd standard. Standard NSpd (three dansyl  
895 groups; Fig. S1(i)) gave an intense  $M+H^+$  signal at  $m/z$  831.30233 ( $C_{42}H_{51}N_6O_6S_3$ ;  
896 0.4 ppm mass error), and a pattern of isotopic signals that match very closely those  
897 predicted for a molecule with this composition. CID-MS-MS of the ion at  $m/z$  831  
898 yielded a product ion spectrum consistent with (dansyl)<sub>3</sub>NSpd (Fig. S1(j)). Panel  
899 (k), product ion spectrum of spot B2 (see panel (a)), identified as DNS-NSpd.  
900 Panel (l), fragmentation diagram of DNS-HSpd. Panel (m), product ion spectrum of  
901 spot F3 (see panel (a)), identified as DNS-HSpd. Component B2 gave a signal at  
902  $m/z$  831.30234 ( $M+H^+$  for (DNS)<sub>3</sub>NSpd; 0.4 ppm mass error) and a product ion  
903 spectrum that identifies this component as NSpd (Fig. S1(k)). Component F3  
904 migrated above DNS-Spd (Fig. S1(a)) and did not correspond with any of the PAs  
905 for which authentic standards were available. Mass spectrometric analysis  
906 generated a strong signal at  $m/z$  859.33357 consistent with  $M+H^+$  for  
907  $C_{44}H_{55}N_6O_6S_3$ , indicating a homologue of Spd with an additional  $CH_2$  group (Fig.  
908 S1(l); 0.4 ppm mass error). The product ion spectrum (Fig. S1(m)) is consistent  
909 with (DNS<sub>3</sub>)HSpd; note that the fragment ions at  $m/z$  541 and 360 in the Spd  
910 spectrum are shifted to  $m/z$  555 and 374 in that of HSpd, consistent with the  
911 presence of an additional backbone  $CH_2$  group. The mass spectrum of a DNS-PA  
912 that migrated similarly to a DNS-Cad standard on HPTLC plates (Fig. S1(a), spot  
913 B1) gave an intense signal at  $m/z$  569.22520 corresponding to an elemental  
914 composition  $C_{29}H_{37}N_4O_4S_2$  ( $M+H^+$  for (DNS)<sub>2</sub>diaminopentane; 0.2 ppm mass error)  
915 and a pattern of isotopic signals matching in relative intensities very closely those  
916 predicted for this molecular composition. The product ion spectrum was not  
917 recorded, and so the substitution pattern was not determined. The identities of

918 DAP and NH<sub>3</sub> were assigned based only on their co-migration with DNS  
919 derivatives of these compounds.

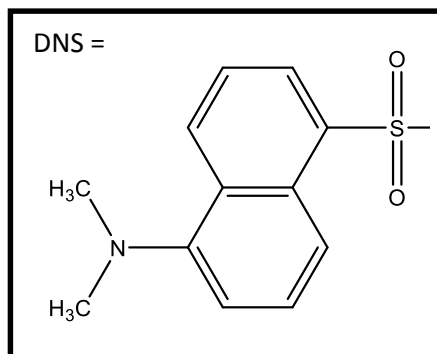
920

921

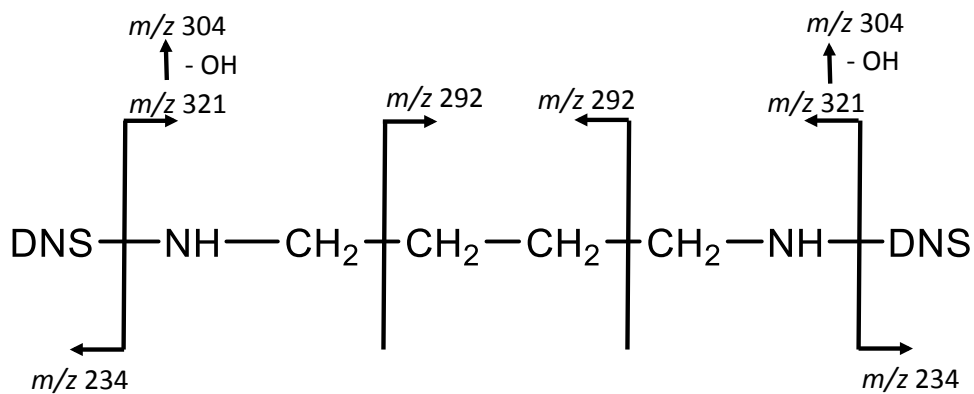
(a)



(b)

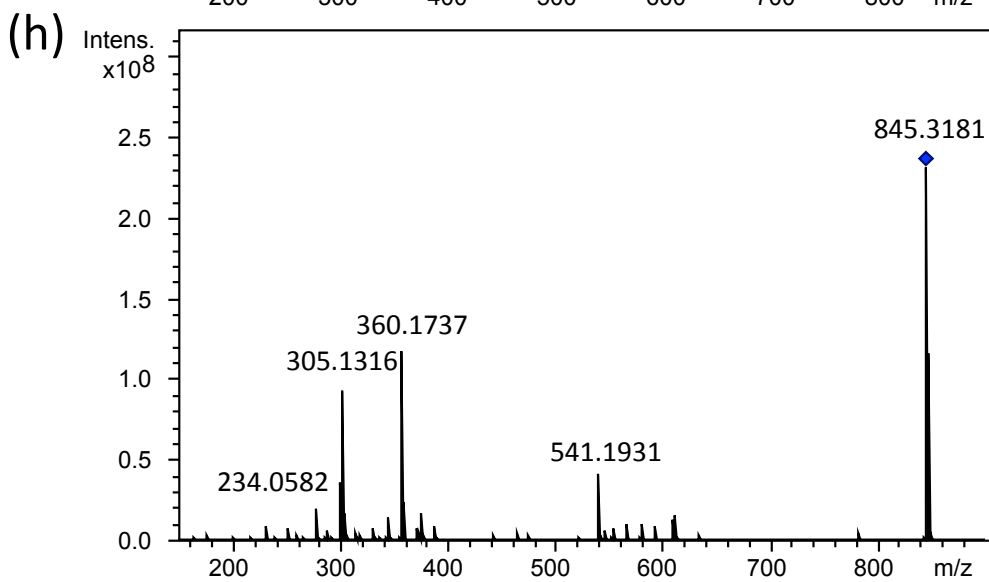
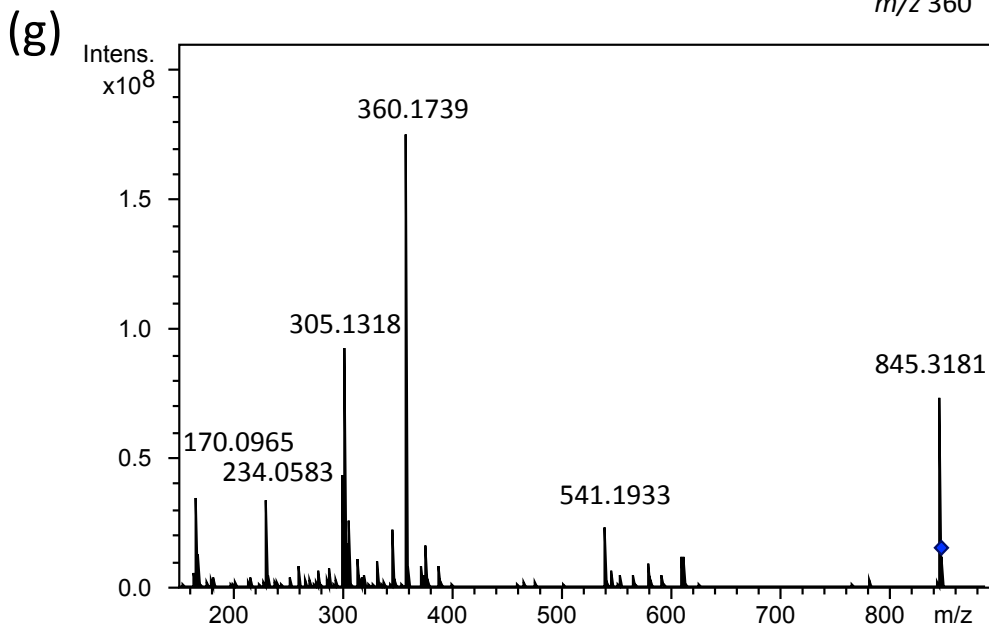
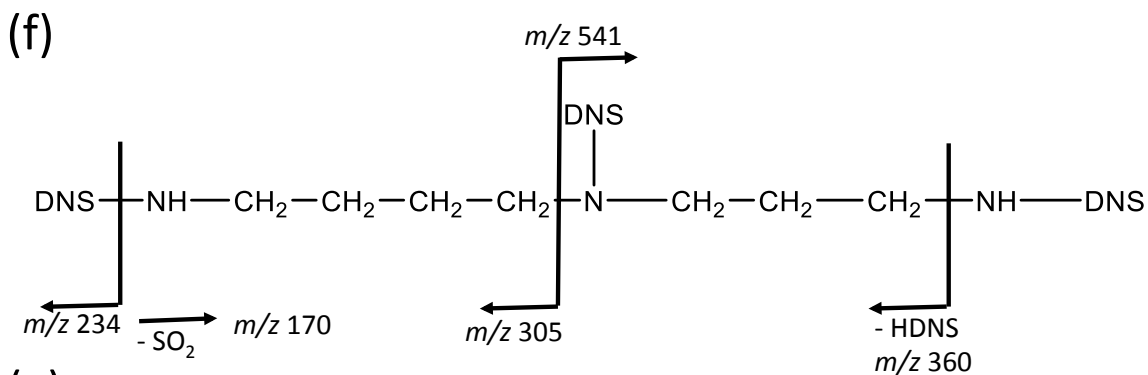


(c)



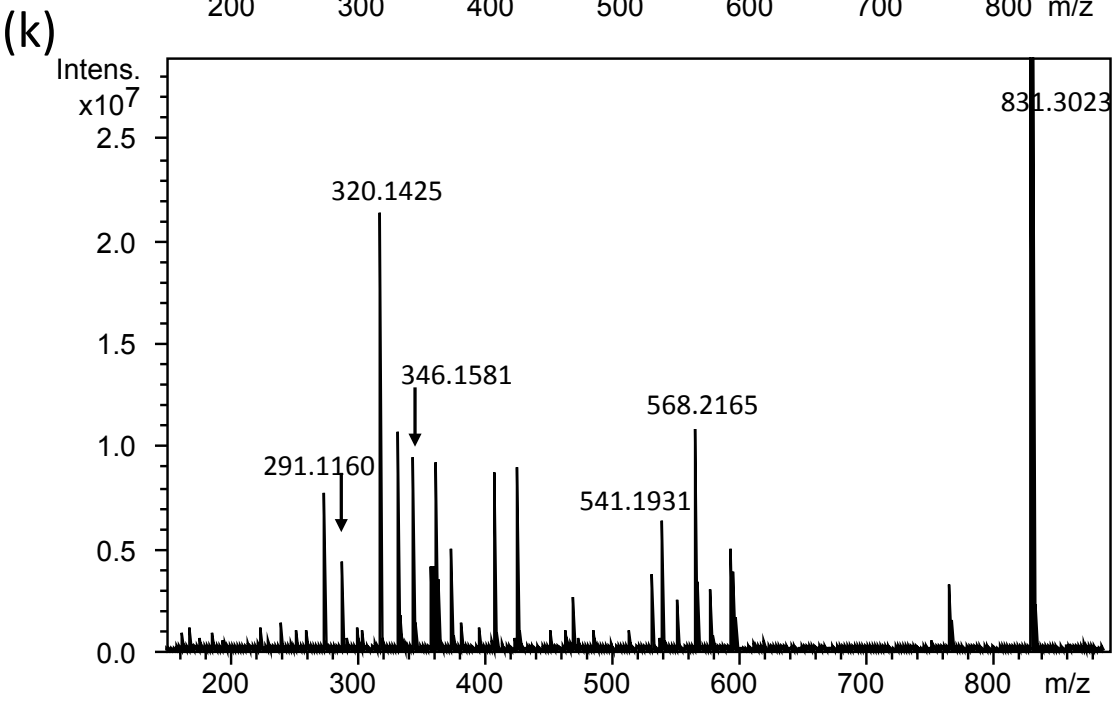
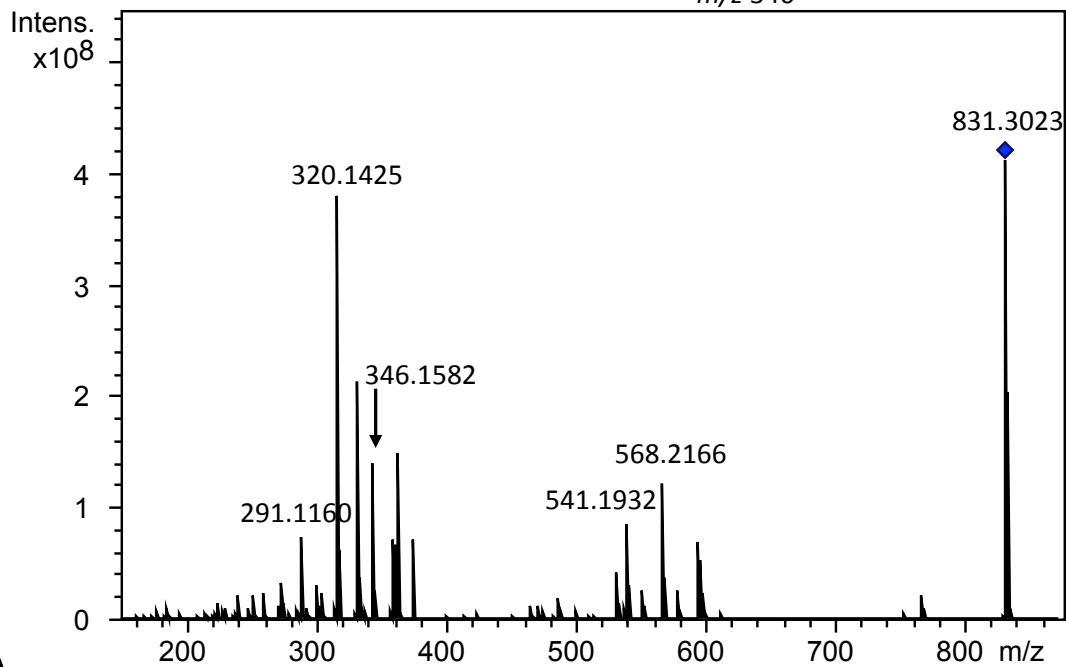
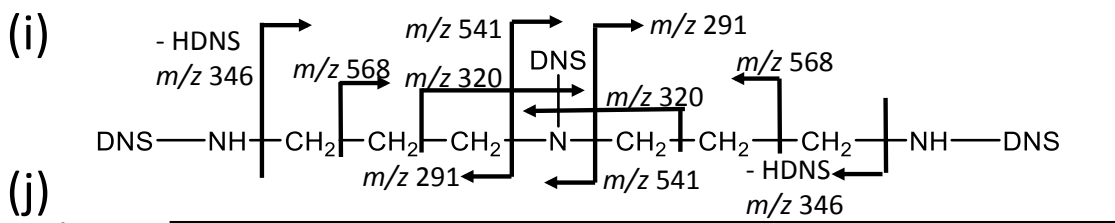
922

923



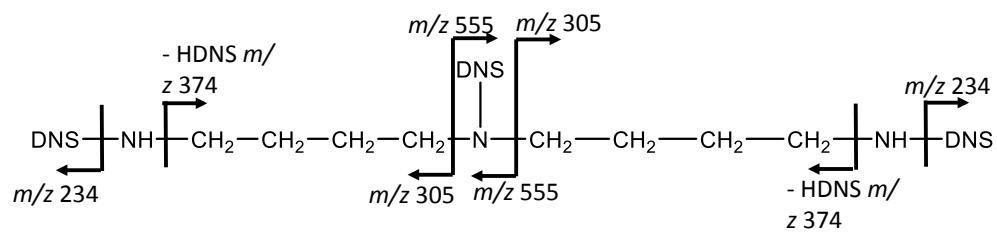
924

925

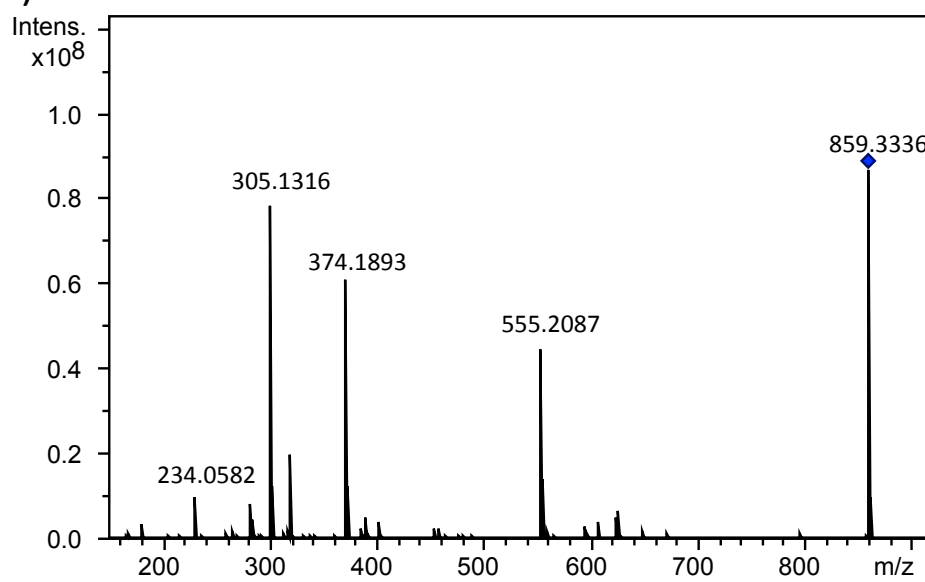


926  
927

(l)



(m)



928

929 Fig. S1

930

931